DYNAMIC RESPONSE OF BATTER PILES CONSIDERING SOIL-STRUCTURE INTERACTION

MD. YOUSUF PASHA

DEPARTMENT OF CIVIL ENGINEERING

BANGLADESH UNIVERSITY OF ENGINEERING AND TECHNOLOGY, DHAKA, BANGLADESH

JULY, 2015

DYNAMIC RESPONSE OF BATTER PILES CONSIDERING SOIL-STRUCTURE INTERACTION

by

MD. YOUSUF PASHA

A thesis submitted to the Department of Civil Engineering of Bangladesh University of Engineering & Technology, Dhaka in fulfillment of the requirement for the degree

of

MASTER OF ENGINEERING IN CIVIL ENGINEERING (STRUCTURAL)

DEPARTMENT OF CIVIL ENGINEERING

BANGLADESH UNIVERSITY OF ENGINEERING AND TECHNOLOGY

JULY, 2015

The thesis titled "**Dynamic Response of Batter Piles Considering Soil-Structure Interaction"**, submitted by **MD.YOUSUF PASHA**, Student Number- **100604322 F,** Session **October 2006,** has been accepted as satisfactory in partial fulfillment of the requirement for the degree of **Master of Engineering (Civil and Structural)** on **28 July 2015.**

BOARD OF EXAMINATION

Dr. Raquib Ahsan — **Chairman (Supervisor)**
Professor
Department of Civil Engineering
BUET, Dhaka-1000

Dr. Mehedi Ahmed Ansary — **Member**
Professor
Department of Civil Engineering
BUET, Dhaka-1000

Dr. Syed Istiaq Ahmad — **Member**
Professor
Department of Civil Engineering
BUET, Dhaka-1000

DECLARATION

I hereby certify that the research work reported in this thesis work has been performed by me and this work has not been submitted elsewhere for any other purpose, except for except for publication

Signature of the Candidate

_____

MD.YOUSUF PASHA

ACKNOWLEDGEMENT

The author wishes to convey his profound gratitude to Almighty Allah for His graciousness, unlimited kindness and blessings and for allowing him to complete the thesis.

I wish to express my profound gratitude to my supervisor Dr. Raquib Ahsan, Professor, Department of Civil Engineering, Bangladesh University of Engineering and Technology. Throughout the duration of the present study, he has given me invaluable guidance, criticism, suggestions, and encouragement. His enthusiasm and expertise were immersed into any little progress on my research work. For all of this, I will always be greatly appreciative.

ABSTRACT

Batter pile groups application has been increased in recent years due to its considerable resistance against lateral loading condition. Actually batter pile groups are more appropriate choice to resist lateral forces due to seismic excitations and inertial forces, because vertical pile group perform much weaker while seismic motions affect these structures.

The objectives of the present study are to evaluate modal behavior of Batter piles at various Batter angles and also to evaluate pier top deformations of Batter pile with respect to free field deformations at different batter angle with different frequencies.

In this study, the pile head stiffness will be determined by the Thin Layered Element Method (TLEM) considering semi-infinite layered soil profile. The substructure i,e. the pile cap along with the pile soil system will be considered such as pile to pile interaction will be ignored. The individual pile stiffness will be considered as complex stiffness. Only stiffness and damping properties will be considered from the substructure. Modal analysis of a viaduct-pile system will be conducted by Mathmatica 5.0 and the kinematic interaction between a viaduct and the pile foundation will be investigated by sub-structure method.

In the present study it has been observed that for low batter angle pier top deformation are in phase and pier top rotation & pile top rotation are out-of-phase but for greater batter angles, the pier top deformation is out of phase and rotations are in phase and anti-clockwise rotations at both pier top and pile cap occur. In the present study it has been observed that in lower frequencies pier goes through almost rigid body motion. Frequency greater than 3.5 Hz, pier top deformations increase. But the rate of change of pier top deformation increases with the increase of batter angle. It has been also observed that in lower frequencies pier top deformation are out of phase and in higher frequencies the same are in phase.

It has been also observed that at resonance frequency there have no significant effect of batter angle on phase difference between pier top and pile cap rotation.

CONTENTS

LIST OF TABLES

LIST OF FIGURES

CHAPTER 1
INTRODUCTION

1.1 General

Batter pile is defined as a pile driven at an inclination to the vertical to provide resistance to horizontal forces. Batter piles are used to transfer inclined load and horizontal forces. In the preliminary design, the load on batter pile is generally considered to be axial. The distribution of load between batter and vertical piles in a group may be determined graphically or by analytic methods. Due consideration should be given to secondary bending as well as pile cap movement, particularly when the cap is rigid.

Batter pile groups application has been increased in recent years due to its considerable resistance against lateral loading condition. Actually batter pile groups are more appropriate choice to resist lateral forces due to seismic excitations and inertial forces, because vertical pile group perform much weaker while seismic motions affect these structures.

Batter piles are usually inclined at an angle of 10° or a slope 1H: 6V. For such mild slope, pile head stiffness of a single batter pile may not differ significantly from that of a vertical pile. However the orientation of the axial and lateral stiffness of a batter pile is inclined by the batter angle. The substructure (i,e. the pile cap along with the pile-soil system) may be modelled with axial and lateral springs substituted for the piles and soil, if pile-to pile interaction can be ignored. Usually pile to pile interaction becomes important for very high frequency. Then pile cap stiffness may be expressed in terms of axial and vertical spring stiffness and the batter angle.

1.2 Objectives of the Study

The principal objectives of the present study are:

- To evaluate modal behaviour of Batter piles at various Batter angles.
- To evaluate pier top deformations of Batter pile with respect to free field

deformations at different batter angle with different frequencies.

1.3 Methodology of work

The pile head stiffness will be determined by the Thin Layered Element Method (TLEM) considering semi-infinite layered soil profile. The substructure i,e. the pile cap along with the pile soil system will be considered such as pile to pile interaction will be ignored. The individual pile stiffness will be considered as complex stiffness. Only stiffness and damping properties will be considered from the substructure.

Modal analysis of a viaduct-pile system will be conducted by Mathmatica 5.0 and the kinematic interaction between a viaduct and the pile foundation will be investigated by sub-structure method.

1.4 Scope of the Study

This study involves the seismic response of the batter pile considering the effect of soil-structure interaction. The following are the scopes of the study:

- Concrete pile is considered in this study but steel pile is not considered.
- Pile-soil interaction is considered but pile-soil-pile interaction is not considered.
- Linear analysis is considered but nonlinear analysis is not considered.
- Frequency domain analysis is performed but time-history analysis is not performed.

CHAPTER 2
LITERATURE REVIEW

The contents of this chapter are taken from a study paper of Ahsan et al [7] named "Analysis of Axial vibration of Piles in layered soil media and application to Batter pile foundations" which is published in "New Technologies for Urban safety of Mega cities in Asia ed: M.H. Ansary and K. Worakanchana, ICUS Report, 2007".

2.1 Introduction

A Semi-analytical approach for solving the problem of interaction of pile with semi-infinite layered soil medium in axial vibration is presented here. The method is similar to the Thin layered Element Method which was originally developed for solving pile-soil interaction problem in lateral vibration. The results are in agreement with other available methods. The effect of Poisson ratio on axial vibration of piles is examined. Then a simplified expression for pile head stillness is derived and compared with the solution of the semi-analytical method for different parameters. Model parameters of pier supported by batter poles is studied for different batter angles. A frequency domain analysis of the pile-pier system considering the kinematics interaction of the poles is performed for horizontal free field motion. Predominant mode of vibration of the system is discussed.

2.2 History about previous studies

In many in land fault induced earthquakes like 1998 Chi-Chi earthquake in Taiwan and 1995 Kobe earthquake in Japan, strong vibration in vertical direction was reported. In the recent 2007 Piles Earthquake at Peru, although not an in land fault induced earthquake rather a near-land tectonic earthquake, strong vertical vibration has also been recorded. The behaviour of structures may be significantly influenced by interaction of supporting pile foundation and soil in axial vibration. Vibratory machines may also induce axial vibration in pole foundations. In the case of batter

piles vibration along the axis of a pile may be induced even in the case of horizontal vibration of soil.

Sheikhbahaei et al told [1] nevertheless the application of these pile groups is effectively restricted in seismic districts so that some of designer engineers do not recommend using batter pile groups in these areas. That is mostly because of large forces developed in cap which makes it more insecure for other further constructions. Gazetas et al [2] have shown that in particular cases application of batter pile groups is very helpful. Also Juran et al [3] conducted a series of centrifuge tests and pseudo static analysis on batter pile and micro pile groups and concluded that increase of pile inclination angle up to a specified value will cause to significant reduction of both deflection and bending moment in cap-pile connection region.

There have been very few studies regarding the effect of axial stiffness of batter piles on structures in the event of horizontal vibration. In one of the early papers on the dynamic behaviour of batter piles Tazoh et al [4] discussed strain distribution along the length and other important features of batter piles through seismic observation and analysis. However, they did not discuss about modal parameters. Ingham et al [5] performed nonlinear dynamic analysis of a bridge bent supported with batter piles but considered only lateral Winkler type springs acting on the batter piles ignoring the coupling effect among the different layers of soil. Rajashree et al [6] also adopted Winkler type lateral springs and a vertical spring at the pile tip for their non-linear analysis of batter piles. Ahsan et al [7] analyzed a pier of an existing old bridge, namely Yanagizawa bridge situated in Shizuoka, Japan with a simple model. Through a frequency domain analysis considering the kinematics interaction of the piles, the mode of vibration of the pier and pile cap for horizontal free-field vibration was also studied.

Substructure method [8] warrants for pile head stiffness for analyzing super structures, simplified expression of pile head stiffness is also required for experimental methods where only the superstructure is physically modelled and reaction of the substructure is fed back into the system. Konagai et al [9] proposed simplified expression of pile head stiffness for lateral vibration. Similar expression of pile head stiffness for axial vibration is presented in the paper of Ahsan et al [7]. There have been very few studies regarding the effect of axial stiffness of batter poles

on structures in the event of horizontal vibration. One of the early papers on the dynamic behaviour of batter piles is by Tazoh et al. [10]. Tazoh et al. discussed strain distribution along the lengthy and other important features of batter pile through seismic observation and analysis. However Tazoh et al. did not discuss about modal parameters. Ingham et al. [5] Performed nonlinear dynamic analysis of a bridge bent supported with batter piles but considered only lateral Winkler type springs acting on the batter piles ignoring the coupling effect among the different layers of soil. Rajashree and Sitharam [6] also adopted Winkler type lateral springs and a vertical spring at the pile tip for their non-linear analysis of batter piles. In the paper of Ahsan et al [7], a pier of an existing old bridge, namely Yanagizawa bridge situated in Shizuoka, Japan has been analyzed with a simple model. The effect of both axial and lateral stiffness of batter piles on the modal parameters of the pier was discussed there. A pier of an existing old bridge, namely Yanagizawa bridge situated in Shizuoka, Japan has been analyzed with a simple model. The effect of both axial and lateral stiffness of batter piles on the modal parameters of the pier was discussed there. Through a frequency domain analysis considering the kinematics interaction of the piles, the mode of vibration of the pier and pile cap for horizontal free-field vibration was also studied.

2.3 Verification and the effect of Poisson ratio

Pile head stiff nesses obtained using the present method is verified with the results obtained by Nogami and Novak [12]. Nogami and Novak solved axi-symmetric equation of vertical motion of a visco-elastic homogeneous medium assuming that there is no horizontal displacement. Pile head stiffness for varying ratios of pile length to pile outer radius and shear wave velocity to longitudinal wave velocity are produced in Figure 2.1. Here Poisson's ratio of 0.4, the ratio of soil density to pile density of 0.6 and damping ratio of 2% is assumed. The curves presented in Fig.2.1 match with the results obtained by Nogami and Novak.

An important feature of the pile head stiffness for axial vibration is that bend a certain frequency the imaginary part increases with increasing frequency. Below that specific frequency the imaginary part remains constant. Around this particular frequency a sudden drop of the real part of stiffness also occurs. Nogami and Novak observed that

this particular frequency is around the resonant frequency of the soil layer. According to their derivation the resonant frequency of soil corresponds to the longitudinal wave velocity. However, according to the present method which is more rigorous than method of Nogami and Novak as Figures 2.1 and 2.3 show, the frequency at which reduction of Poisson' ratio Figure 2.2 shows the pile head stiffnesses of the same pile with soil media having the same longitudinal wave velocity but different Poisson's ratio and thus different shear modulus. It can be observed from the figure that as the Poisson's ratio increases the frequency at which real part of stiffness drops or the imaginary part of stiffness starts increasing deviates from the resonant frequency of soil corresponding to longitudinal wave velocity. As the Poisson's ratio increases the media tends to become incompressible and the dilational wave becomes less predominant in axi-symmetric vibration. Nogami and Novak mentioned that in contrast to plain strain case, Poisson's ratio does come into play in their solution but basically due to change in shear modulus. They did not elaborate on the change of mode of wave propagation due to change in Poisson's ratio.

Yang and Sato [13] reported that during 1995 Kobe earthquake the predominant average vertical wave velocity, as measured in an array site at Port island on the southwest side of Kobe city, was very low (around 590m/s). They reasoned that the low vertical wave velocity is due to the reduction in P-wave velocity for incomplete saturation. However the results of the present analysis indicate that the predominant vertical wave velocity may be low since P-wave becomes less predominant in saturated soil even in axi-symmetric vibration. Figure 2.3 shows that the change in pile head stiffness with frequency is very small for varying Poisson's ratio and subsequently for varying P-wave velocity when the shear modulus of soil is constant.

2.4 Pile head axial stiffness

In order to study the interaction between the superstructure and the substructure of embedded pile, the solution of the present method must be combined with the model of superstructure. Usually this done by the Method of Sub structuring, where the superstructure is modelled numerically or a physical model of superstructure is tested and the effect of substructure is introduced with some impedance function. In most of the applications this impedance function is preferred to be as possible.

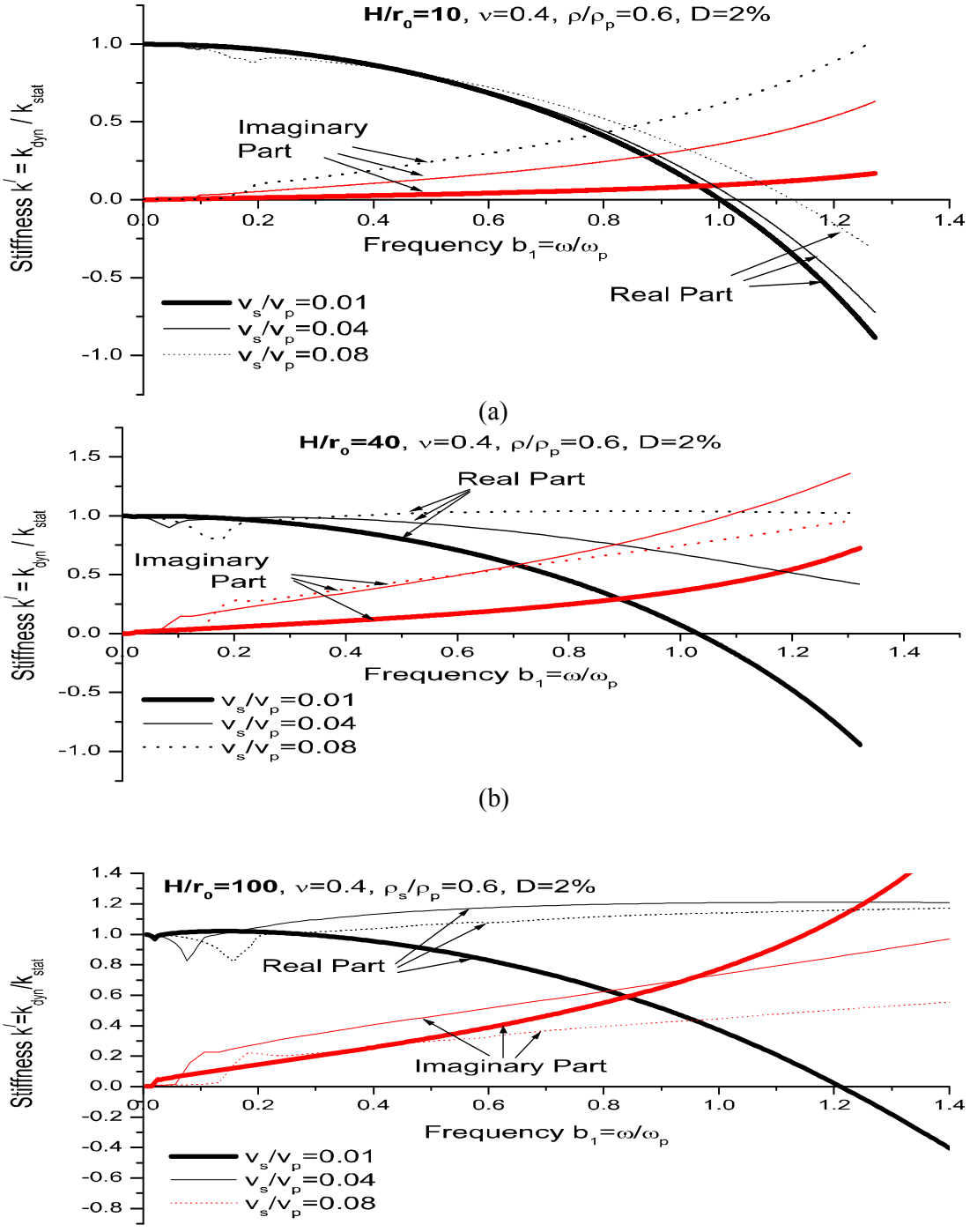

Figure 2.1: Variation of normalized pile stiffness with frequency and soil stiffness (a) very short pile, (b) moderately slender pile, (c) slender pile

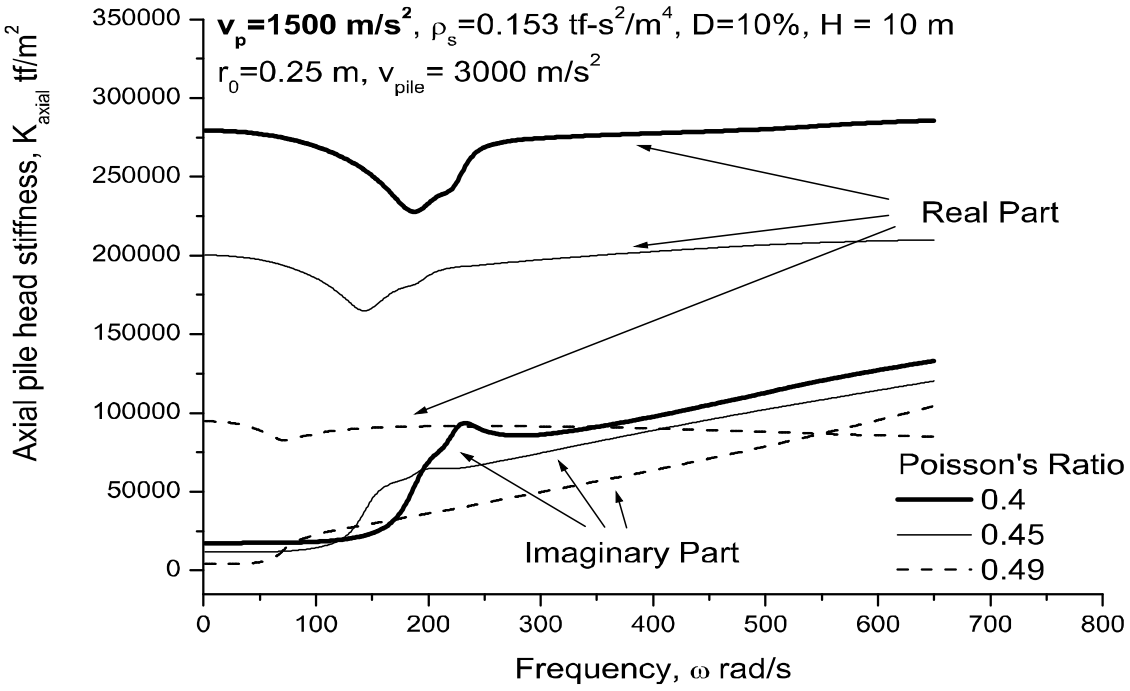

Figure 2.2: Axial pile head stiffness for same longitudinal velocity of soil media with different Poisson's ratio.

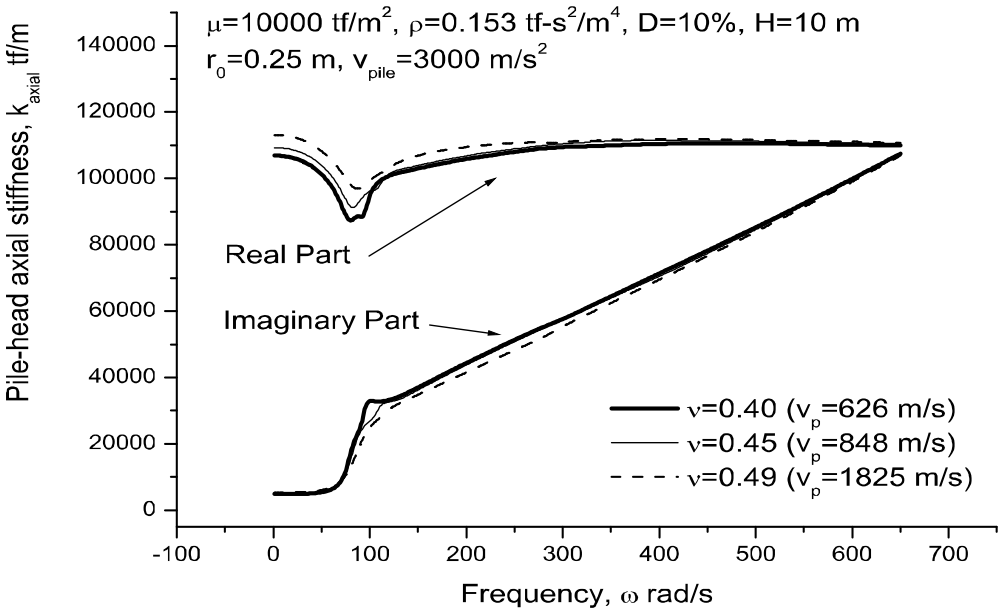

Figure 2.3: Axial pile head stiffness for same shear modulus of soil with different Poisson's ratio.

This is particularly true for experiments the superstructure is physically modelled and the effect of substructure is simulated in real time with a transfer function. Some representative cases are shown in figures 2.4-2.10.

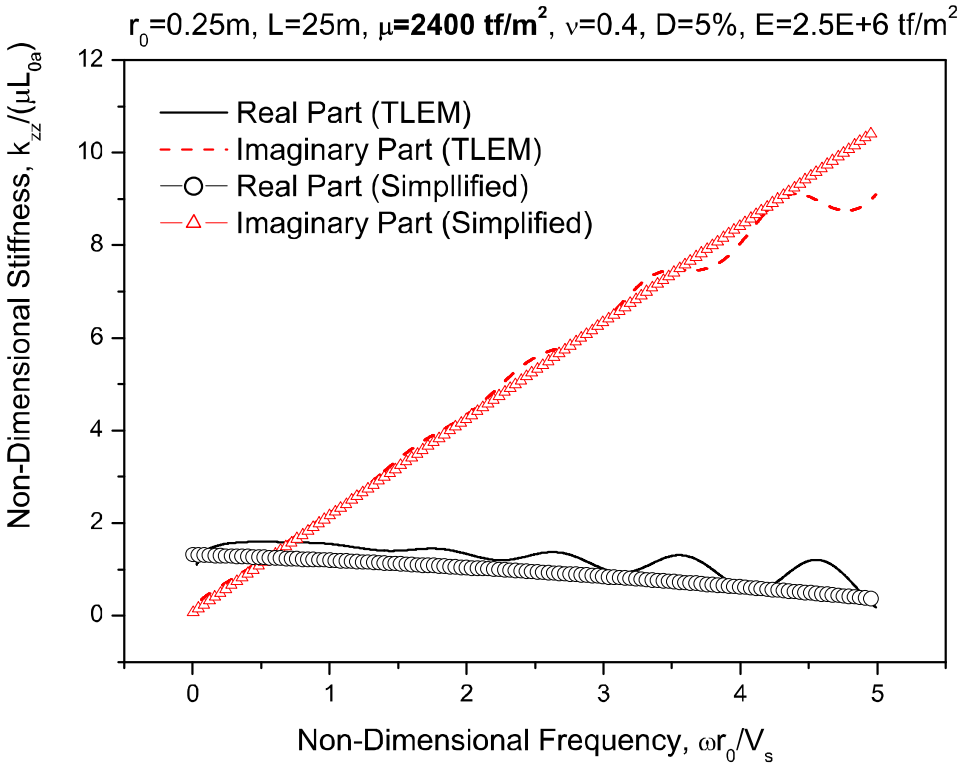

Figure2.4: Variation of axial stiffness of pile head with frequency (μ=2400 tf/m^2).

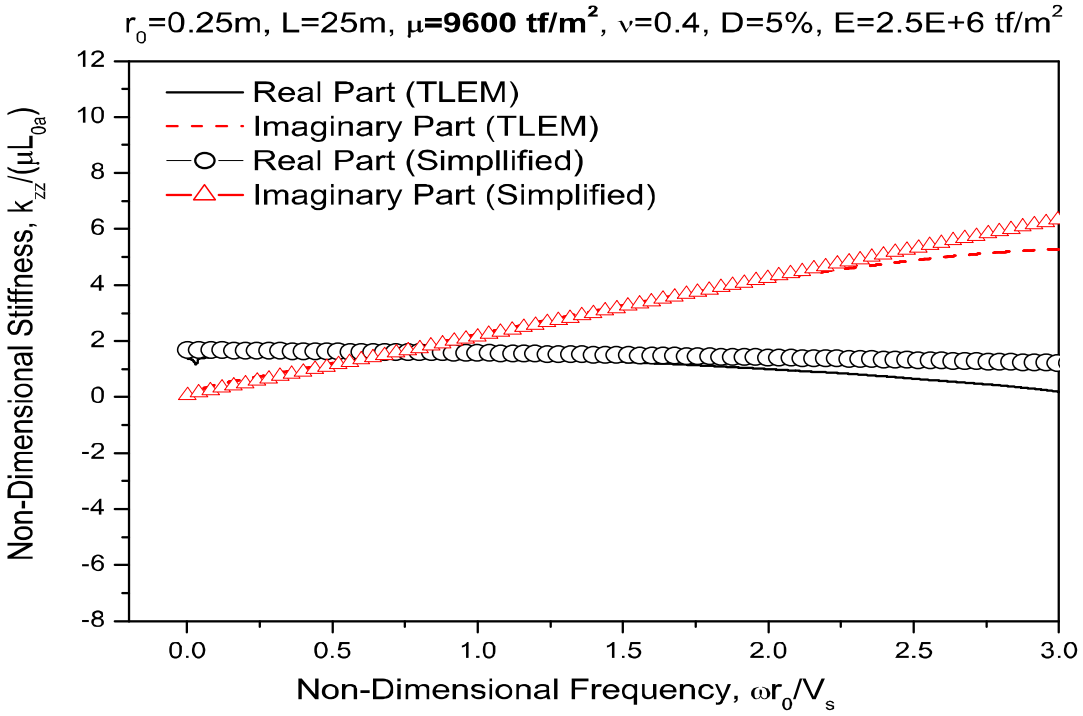

Figure 2.5: Variation of axial stiffness of pile head with frequency (μ=9600 tf/m^2).

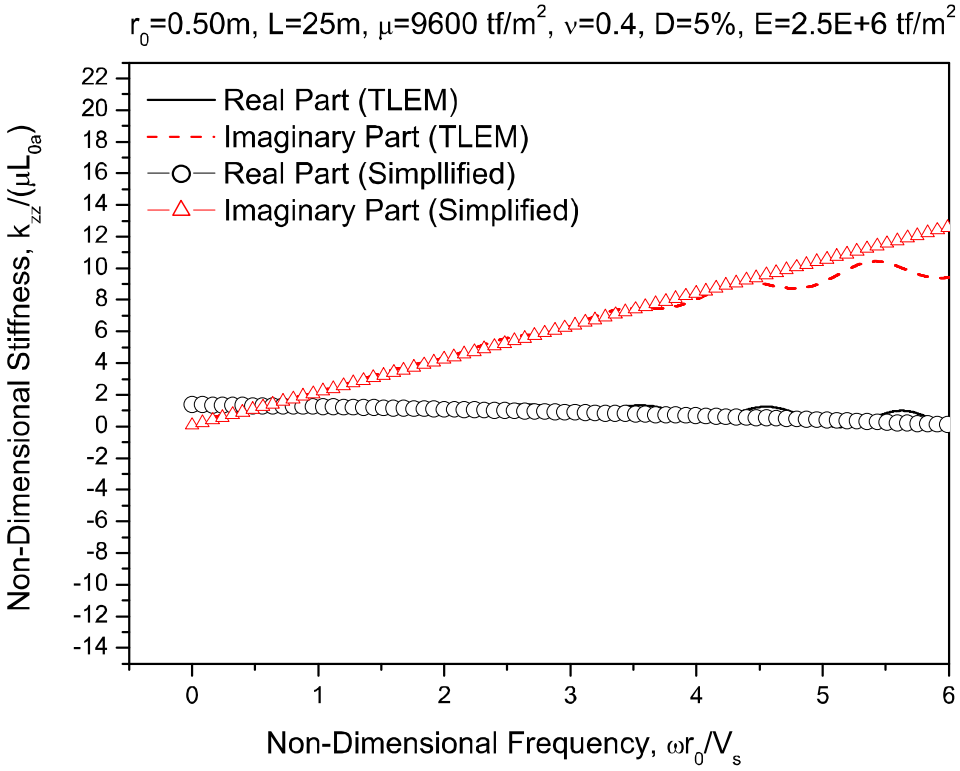

Figure 2.6: Variation of axial stiffness of pile head with frequency (r_0= 0.5m)

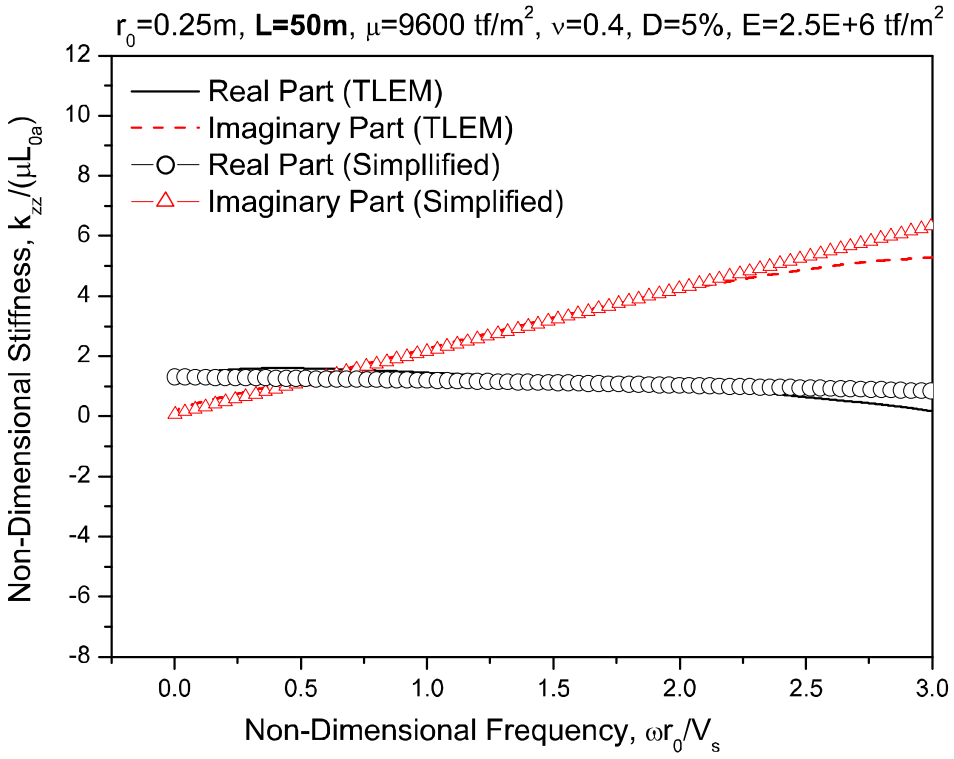

Figure 2.7: Variation of axial stiffness of pile head with frequency (L= 50 m)

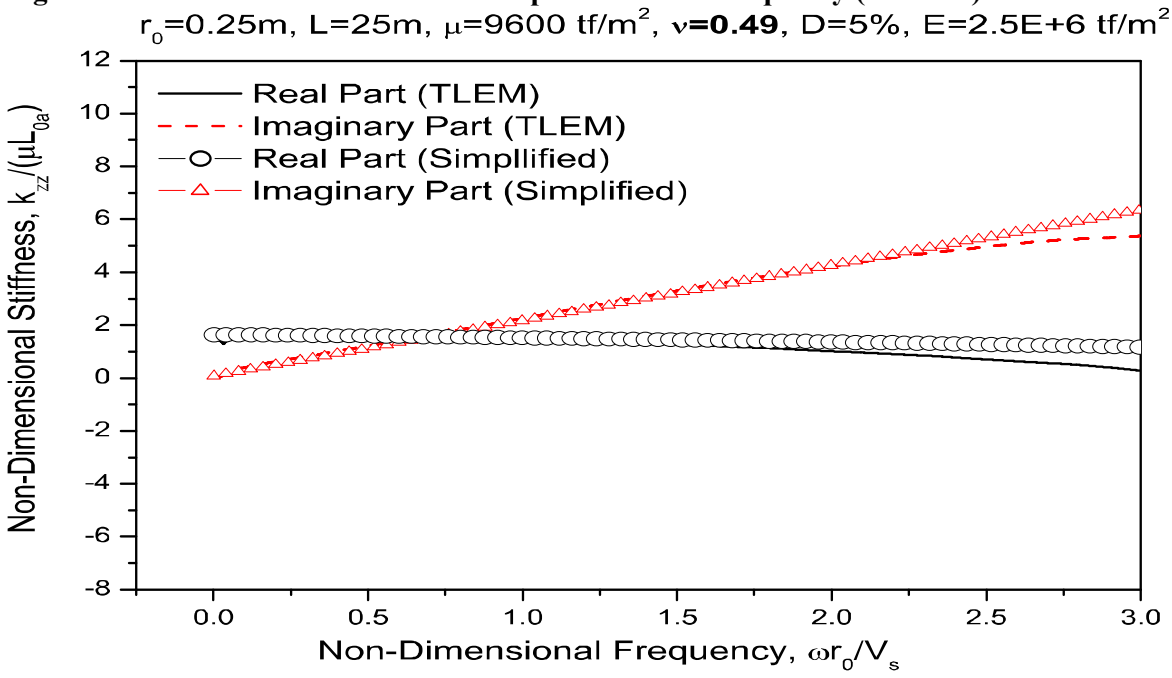

Figure 2.8: Variation of axial stiffness of pile head with frequency (υ= 0.49)

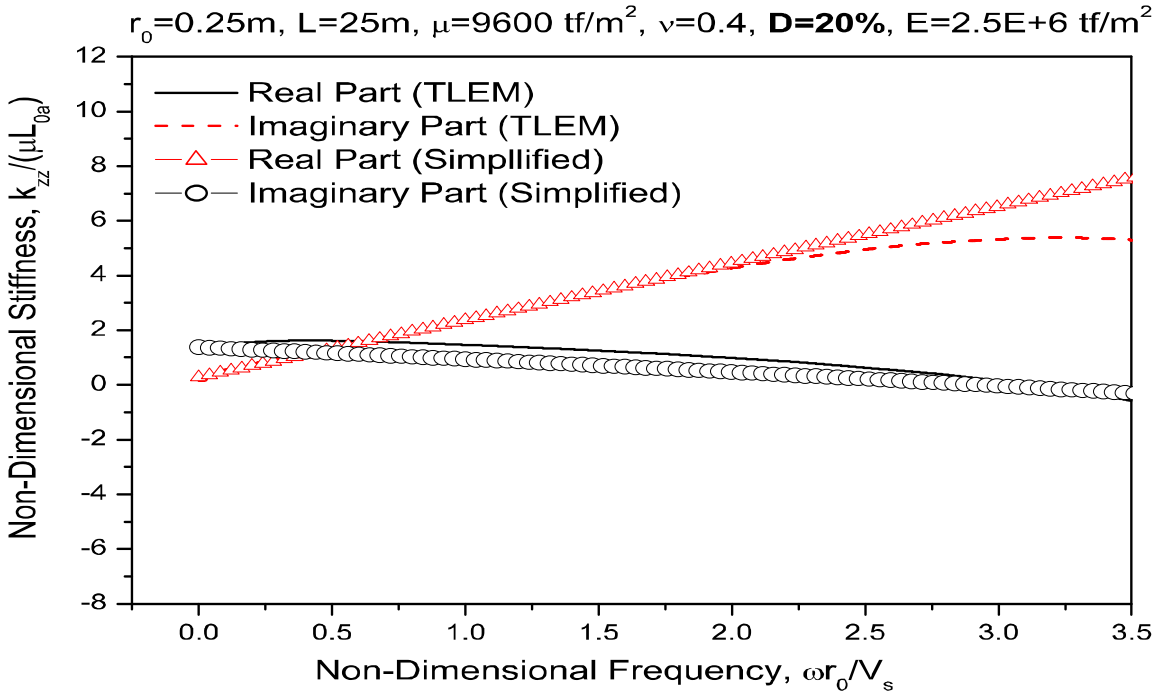

Figure 2.9: Variation of axial stiffness of pile head with frequency (D= 20%)

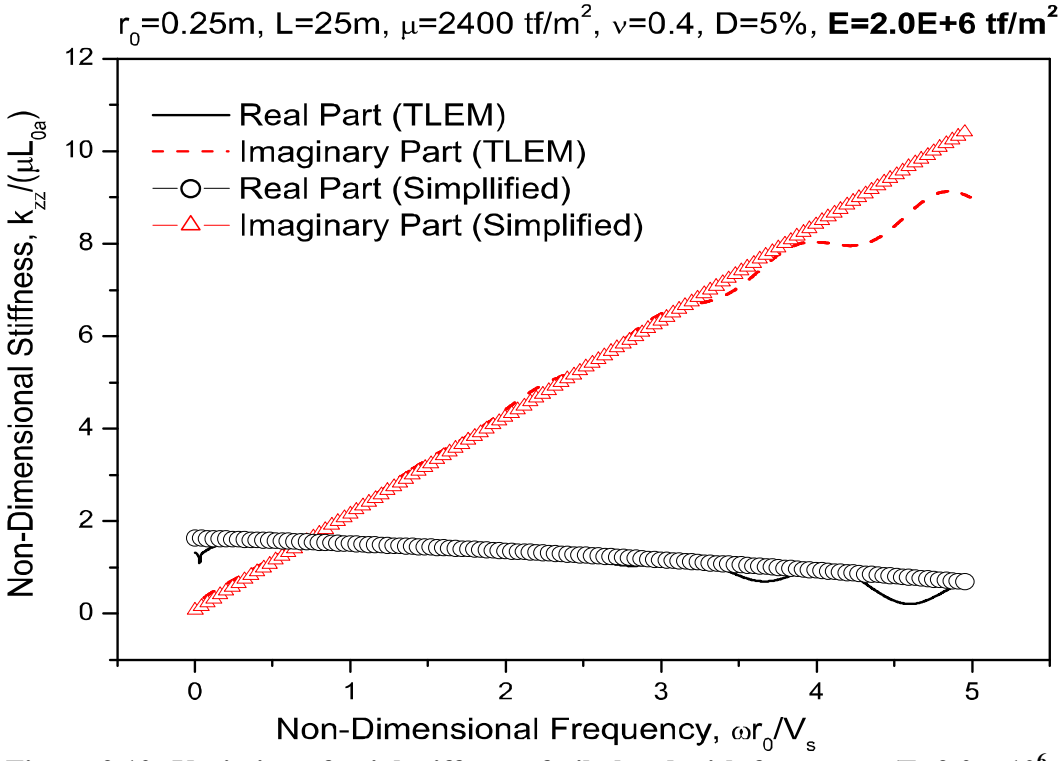

Figure 2.10: Variation of axial stiffness of pile head with frequency (E=2.0 x 10^6 tf/m^2)

2.5 Modal analysis of a pile-pier system of the Yanagizawa bridge

The method was applied [7] for the pier-pile system of the Yanagizawa Bridge which is located in Tokai region at midway between Tokyo and Osaka in Japan. The bridge was designed in accordance to pre-1995 codal provisions. In apprehension of a major earthquake in Tokai region Japan Railway intends to both vertical and batter piles (Figure 2.11) the piles are steel piles with 254 mm outside diameter and 9 mm thickness. Shear wave velocities of soil at different depths at the site are given in table 2.1. However there is no information available regarding exact length of the piles or whether they reached the bed rock. In order to determine the dynamic behavior of a typical pier-pile system of the Yanagizawa bridge. Figures 2.12and 2.13 show FFT of the records at a pile cap and a cross girder of a pier- along the longitudinal and transverse directions respectively. In each of these records two predominant frequencies are observed one near 0.6 Hz. in both transverse vibrations. The 0.5 Hz. for longitudinal vibration and near 2.4 Hz. for transverse vibration. Frequency of the underlying soil and the second peak is is due to the contribution from the superstructure. The method of modal analysis described in Section 3.2 can determine the modes governed by the dynamical system rather only the stiffness and damping properties are considered from the substructure, the predominant mode of vibration of the underlying soil and the fundamental frequency of soil vibration are not reflected in the present model. The mode of vibration of the pile-pier system at 0.5 Hz. is discussed in Section.

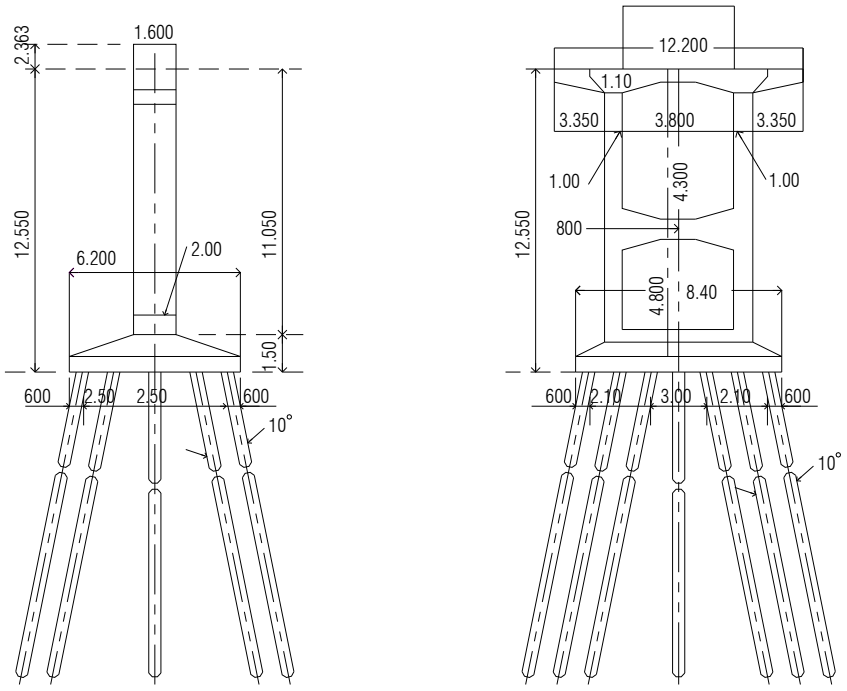

Figure 2.11: Typical pier-pile assemblage of Yanagizawa viaduct

Depth (m)	Shear wave velocity (m/s)
0-105	113
1.5-8.0	82
8.0-19.0	76
19.0-25.0	61
25.0-31.0	81
31.0-41.2	116
41.2-	510

Table: 2.1 Soil profile at the site of Yanagizawa bridge

A typical pile-pier system of the bridge has been analyzed using the simple model. At first the dynamic stiffnesses, both lateral and axial, of a single upright beam have been calculated for the specific site characteristics. Lateral and axial impedances of a single pile are presented in Figures 2.14 and 2.15. Implementing these pile head impedances for each pile for the given pile arrangement. Since the exact length of the piles are unknown, it was assumed that the piles extend down to 44 m. The results of the modal analysis show that the lowest modal frequency is 1.32 Hz for longitudinal vibration and 2.32 Hz. for transverse vibration. The modes of vibration at these frequencies are schematically shown in Figures 2.16 and 2.17. All the displacement and rotational degrees of freedom are nearly in-phase. The mode shows greater deformation at the pier top and clockwise rotation for rightward motion. The mode is most likely to be induced in case of load acting at the pier top e,g, wind load. As has been explained earlier these modes actually correspond to the second peaks of the frequency spectrums shown in Figures 2.12 and 2.13. However for longitudinal vibration the predominant frequency determined by the modal analysis is much lower than the second peak of Figure 2.12. Reason is probably the present 2D configuration. Thus this 2D model is not appropriate for longitudinal vibration. On the other hand, the predominant frequency in the transverse direction as obtained by the modal analysis matches very well with the second peak of Figure 2.13. Since the torsion rigidity of the deck and longitudinal girders ate insignificant compared to the flexural stiffness of the pier, the 2D model could simulate the dynamic behaviour of the system in transverse direction. Hence, the present 2D model should be used only to discuss vibration.

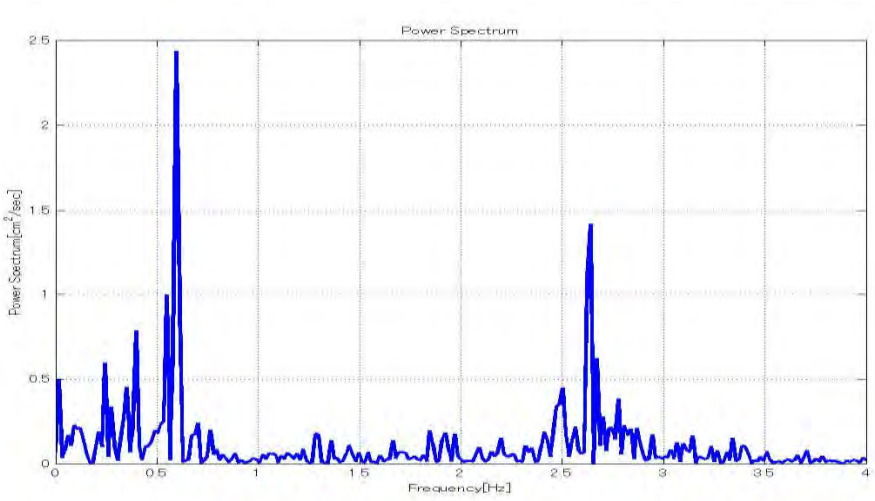

Figure 2.12: Fourier spectrum of the ambient vibration record in the longitudinal direction measured at the cross-girder of the Yanagizawa Bridge.

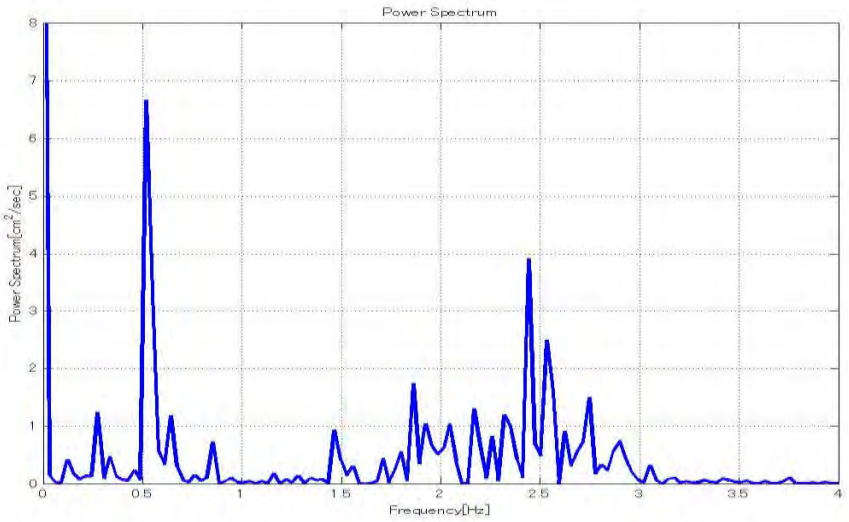

Figure 2.13: Fourier spectrum of the ambient vibration record in the transverse direction measured at the cross-girder of the Yanagizawa Bridge.

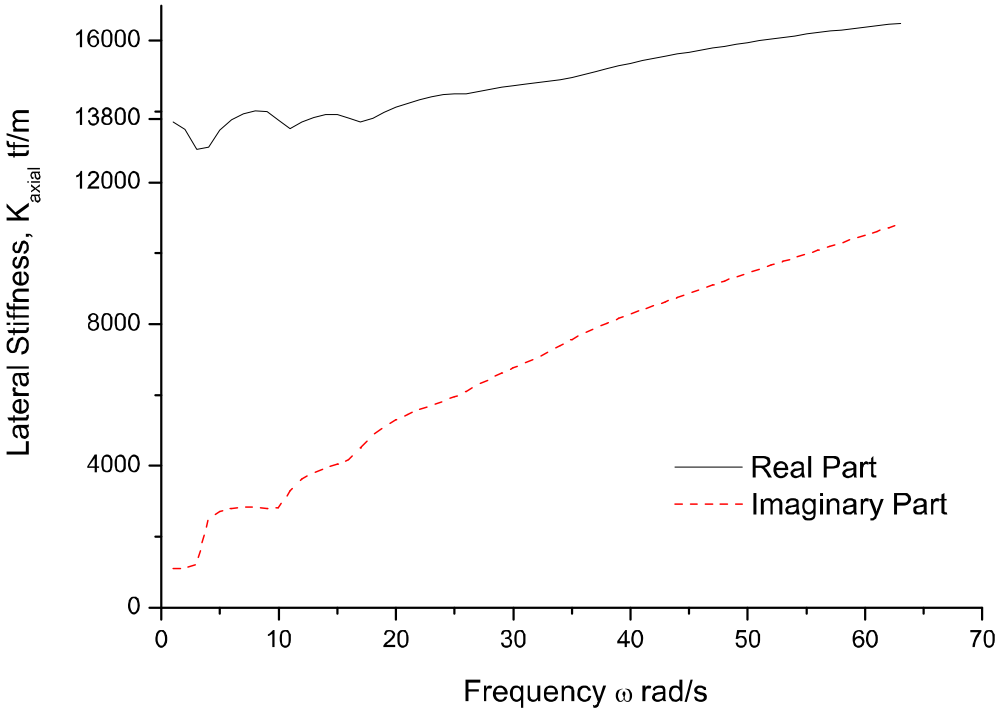

Figure 2.14: Lateral stiffness of a single pile of Yanagizawa Bridge

To understand the effect of the inclination of the batter piles in transverse vibration, modal analyses have been performed for the same pile-pier system with different batter angles of piles. The results have produced in Figure 2.18. From the Figure it is evident that the batter angle has very little effect on the predominant frequency of the system. The modal deformations i.e. the pile cap deformation. pile cap rotation and pier top rotation for unit deformation of the pier top are normalized with those for all vertical pile arrangement and then plotted with increasing batter angle in Figure 2.18. The all vertical pile arrangement has similar mode as shown in Figure 2.17 with slightly different values of modal deformations. pile inclination has the most prominent effect on pile cap deformation. With the increase in batter angle the piles cap the pile cap to deform less. For a certain batter angle between 15 ° and 20° the pile cap deformation in the first mode of vibration becomes zero. Beyond this particular batter angle the pile cap deformation again increases and actually becomes out –of- phase with the pier top and pile cap deformations are in phase and rotations at both the nodes are out-of-phase with the deformations. Thus a right ward pile cap deformation is associated with a right-ward pier top deformation and clockwise rotations at both the nodes. For greater batter angles, however, the pier top

deformation is out of phase and rotations are in phase with pile cap deformation and anti-clockwise rotations at both pier top and pile cap (Figure 2.20) Thus for higher batter angles the mode of vibration induced by a force at the pile cap or ground vibration becomes predominant.

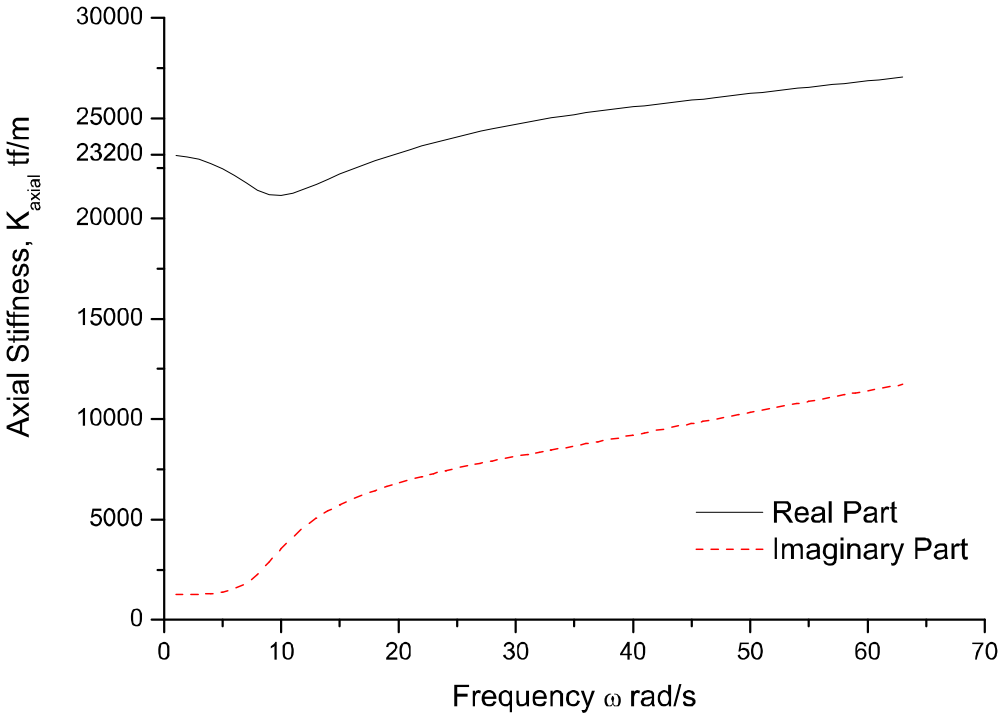

Figure 2.15: Axial stiffness of a single pile of Yanagizawa Bridge

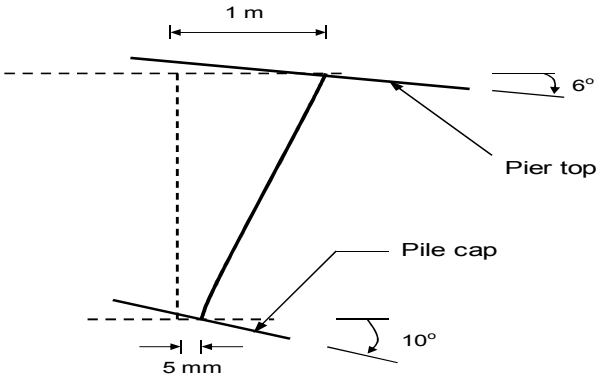

Figure 2.16: Fundamental mode shape of a typical pile-pier system of the Yanagizawa Bridge (not in scale)

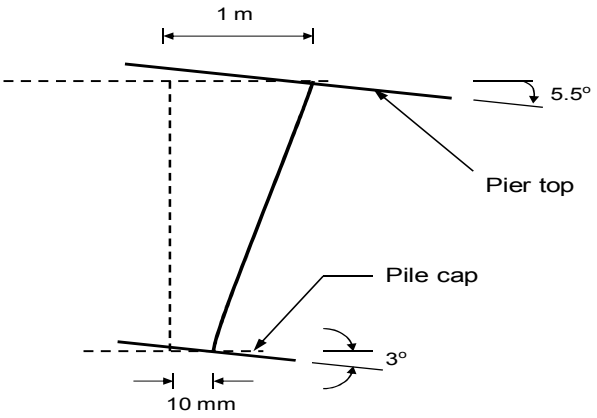

Figure 2.17: Fundamental mode shape of a typical pile-pier system of the Yanagizawa Bridge (not in scale)

3.3 Kinematic interaction

The first peak of Figure 2.13 is due to the predominant frequency of the underlying soil and the response of the structure may be discussed by applying pile cap vibration in the transverse direction.

The inability of an embedded pile foundation to conform to the deformation of soil causes the motion of the soil structure interface to deviate from the free-field motion. The foundation input motion should be modified to incorporate this deviation due to the kinematic interaction. The foundation input motion for the Yanagizawa bridge piers is estimated rigorously by the Thin Layered Element Method (1976). Figures 2.21, 2.22 and 2.23 show the kinematic interaction factors for motions in different directions. Thus without the presence of a superstructure, a horizontal free-field motion would cause a horizontal displacement and a rotation of the pile head producing forces at the pole head.

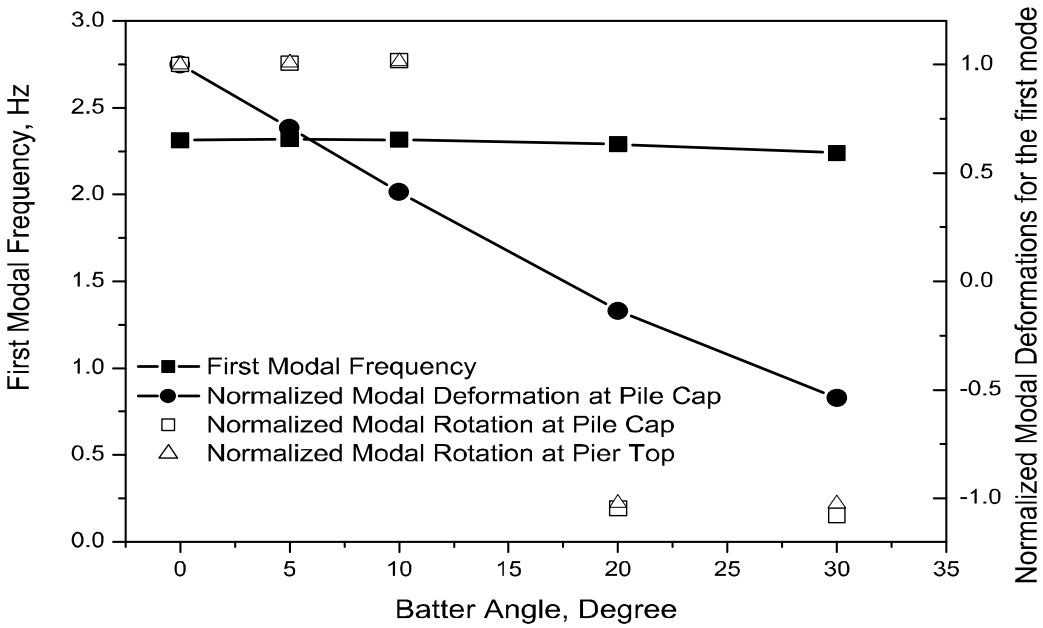

Figure 2.18: Variation of modal parameters of pile-pier system with batter angle

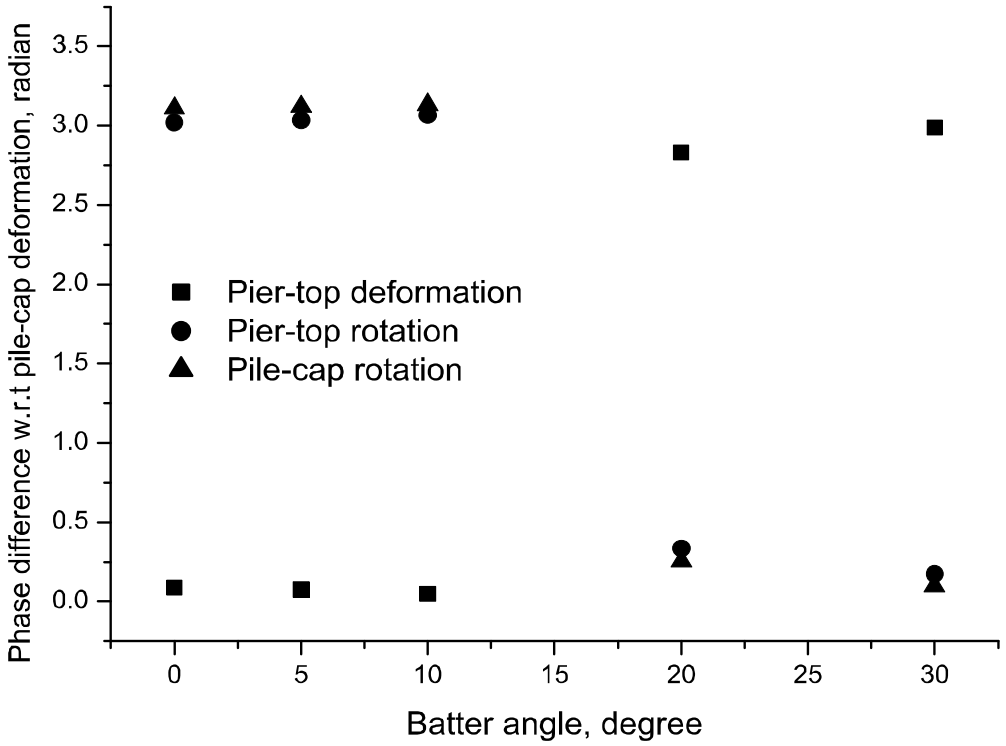

Figure 2.19: Phase difference of modal deformations with respect to pile cap deformation.

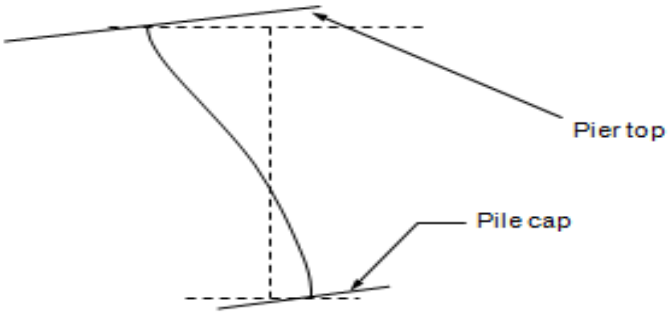

Figure 2.20: First mode of vibration for higher batter angles

Figure 2.24 shows the vibration mode of a typical pier-pile system of the Yanagizawa Bridge at 0.5 Hz for transverse vibration. At this particular frequency cap as the soil deformation occurs to the pile cap rotates counter clockwise; where as the pier top is out of phase rotating in clock wise direction with negligible horizontal translation.

With increasing frequency pile cap deformation increases along with pile cap and pier top rotations (shown in Figure 2.25) these three quantities are always exactly in phase i.e., a right ward pile cap deformation is associated with counter clockwise rotations. This fact was also observed by Tazoh et.al. (1988) from their seismic records at a road bridge, supported by batter piles, in Kanagawa, Japan. It was also reported that the counter clockwise rotation of the footing to a motion to the right continued for the entire duration of the 1983 Kanagawa-Yamanashi- Kenzai Earthquake which had dominant frequencies between 0.5 Hz. to 5 Hz. Thus the present analysis is in agreement with the seismic observation.

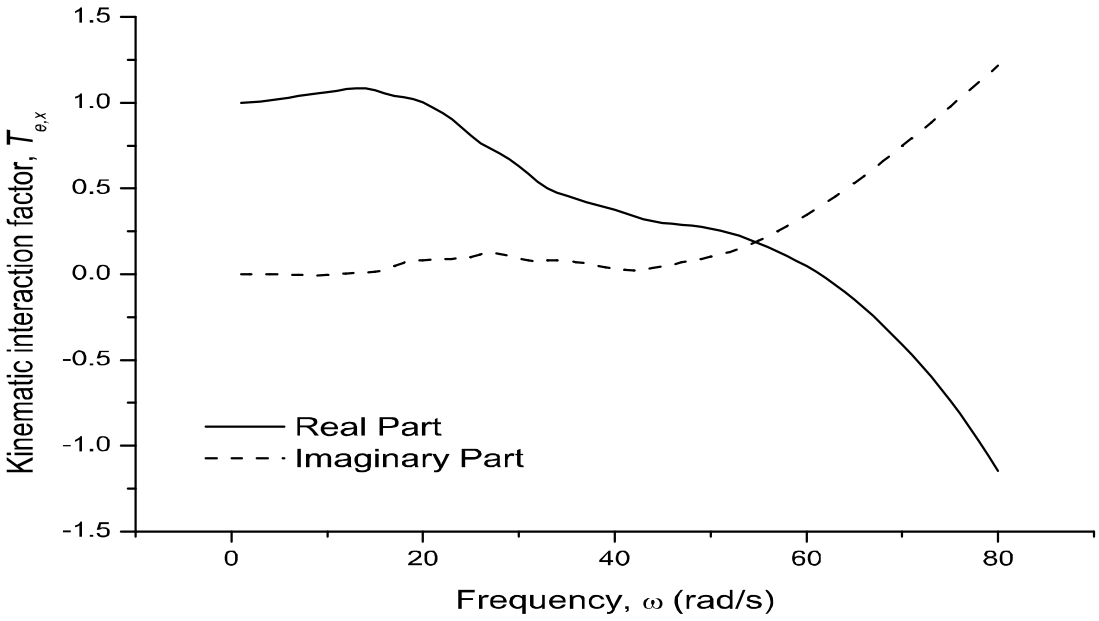

Figure 2.21: Kinematic interaction factor in horizontal direction for horizontal input motion.

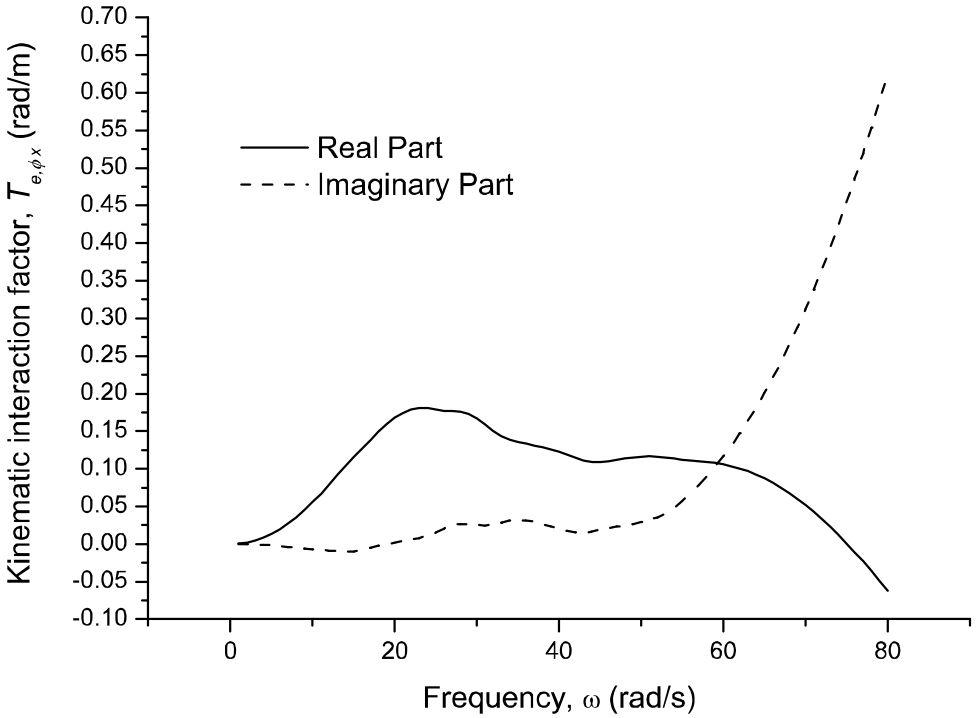

Figure 2.22: Kinematic interaction factor in rotation for horizontal input motion.

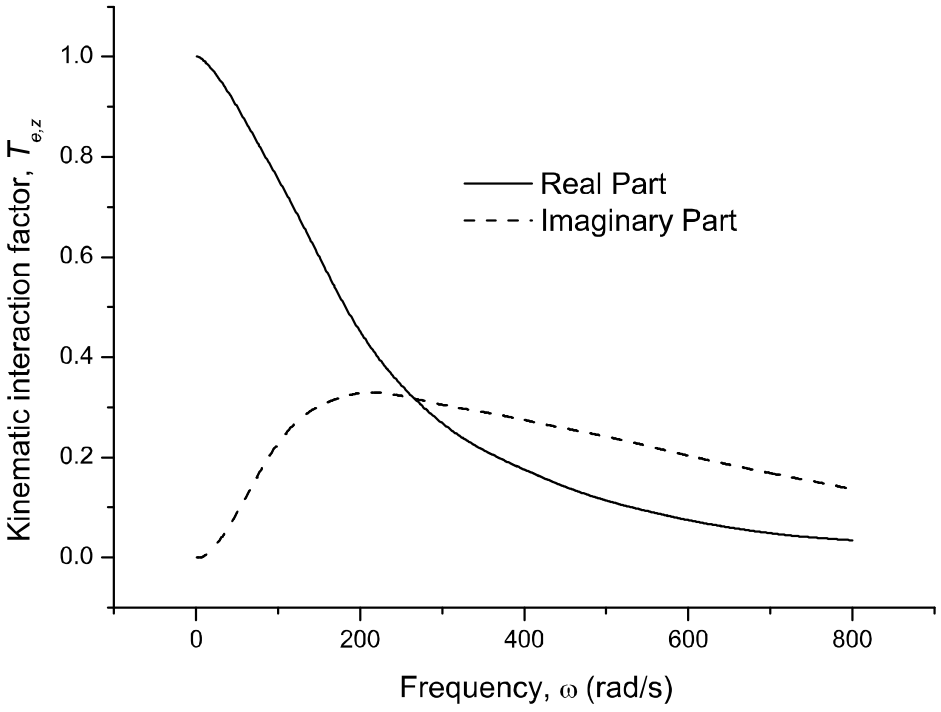

Figure 2.23: Kinematic interaction factor in vertical direction for vertical input motion

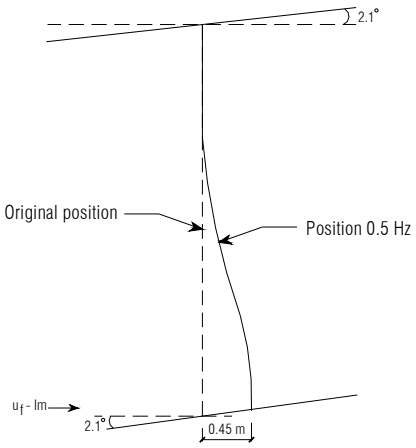

Figure 2.24: Vibration of a typical pile-pier system at the Yanagizawa bridge.

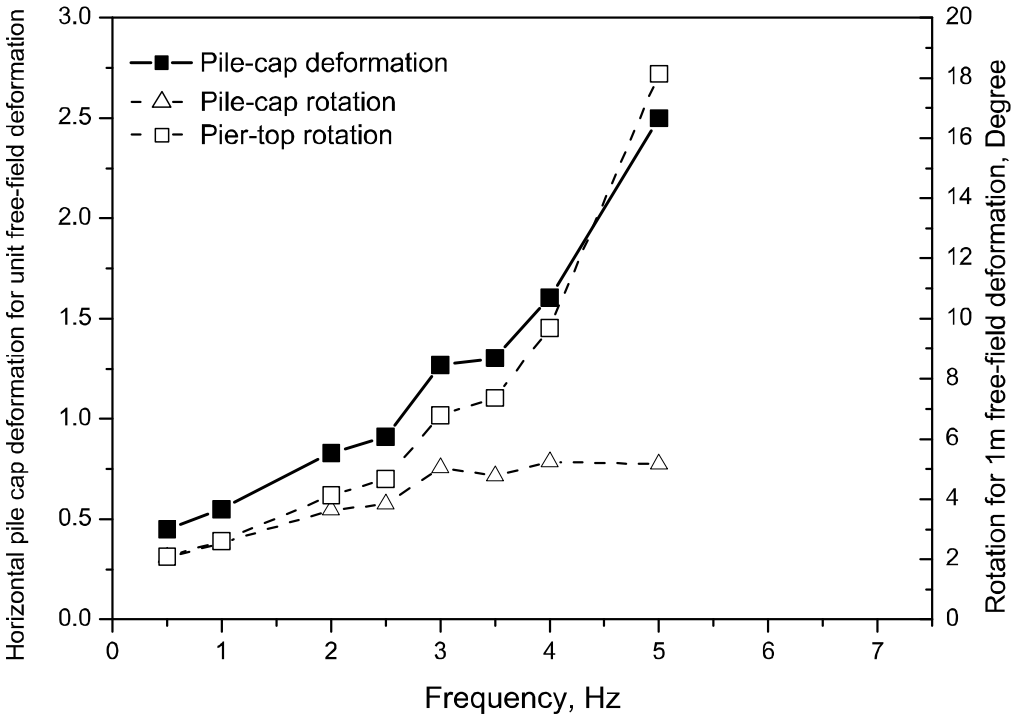

Figure 2.25: Pile cap deformation and pile cap and pier top rotations at different frequencies.

Figure 2.25 shows that pile cap deformation exceeds free –field deformation at around 2.5 Hz. The rate of increase of pier top rotation is more than that of pile cap rotation and may become significant from serviceability point of view in case of higher frequency vibration. pier top deformation is very small compared to pile cap deformation (Figure 2.26). In fact the stiffness of the pier is much greater compared to the mass that in lower frequency the pier goes through almost rigid body motion. For frequencies greater than 3.5 Hz. pier top deformation increases. For lower frequencies pier top deformation is out-of-phase with pile cap deformation. As the frequency increases the two deformations become more in –phase.

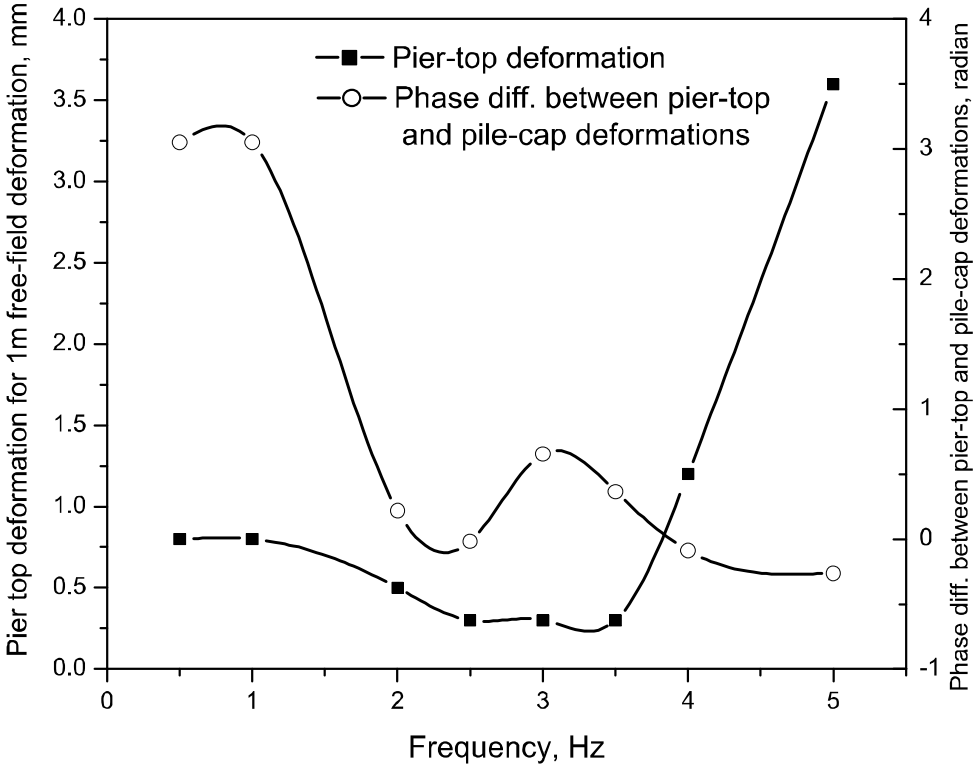

Figure 2.26: Pier top deformation and its phase difference with pile cap deformation at different frequencies.

CHAPTER 3

FORMULATION

The contents of this chapter are taken from a study paper of Ahsan et al [7] named "Analysis of Axial vibration of Piles in layered soil media and application to Batter pile foundations" which is published in "New Technologies for Urban safety of Mega cities in Asia ed: M.H. Ansary and K. Worakanchana, ICUS Report, 2007".

3.1 Axial vibration of a pile in semi-infinite layered soil

In this formulation soil is considered horizontally layered and semi-infinite in lateral extent (Figure 3.1). The soil has fixed boundary at the bottom end of the pile length. First the stiffness equations for deformation along a cylindrical hollow of the same size of a pile in axi-symmetric vibration of soil is formulated. Then axial stiffness of a pile is considered assuring that the there is no slip between soil and pile.

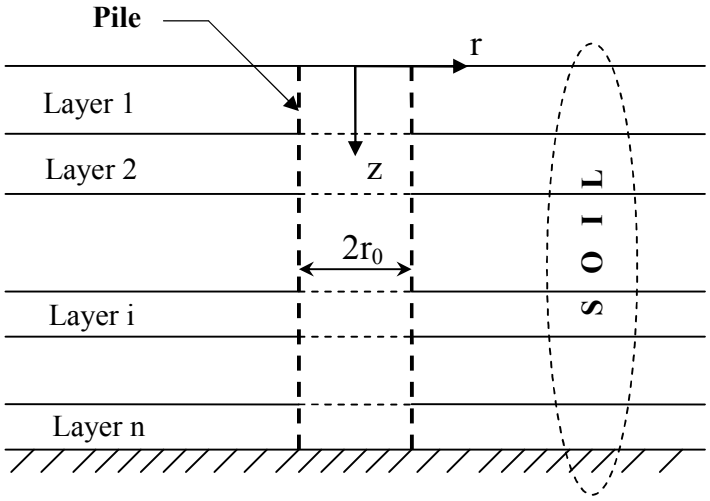

Figure 3.1: Pile-soil model

If u_r and u_z are respectively the displacements in radial and vertical directions, wave motion equations in cylindrical coordinates for an axi-symmetric problem are given by,

$$(\lambda + 2G)\frac{\partial \theta}{\partial r} + 2G\frac{\partial \varpi_0}{\partial z} = p\frac{\partial^2 u_r}{\partial t^2} \tag{3.1}$$

$$(\lambda + 2G)\frac{\partial \theta}{\partial z} - \frac{2G}{r}\frac{\partial}{\partial r}(r\varpi_0) = \rho\frac{\partial^2 u_z}{\partial t^2} \tag{3.2}$$

Where the Lames constants λ and G are complex numbers in order to take material hysteretic damping into account and ρ is the mass density. The dilation θ and rotation ϖ_o are given by,

$$\theta = \frac{1}{r}\frac{\partial}{\partial r}(ru_r) + \frac{\partial u_z}{\partial z}$$

and $$2\varpi_o = \frac{\partial u_r}{\partial z} - \frac{\partial u_z}{\partial r}$$

Let us assume the potential functions for the displacement components of soil as,

$$\begin{Bmatrix} u_r \\ u_z \end{Bmatrix} = \begin{Bmatrix} v_r \\ v_z \end{Bmatrix} e^{i\omega t}, \begin{Bmatrix} v_r \\ v_z \end{Bmatrix} = \begin{bmatrix} H_1^{(2)}(\alpha r) & 0 \\ 0 & H_0^{(2)}(\alpha r) \end{bmatrix} \begin{Bmatrix} \phi(z) \\ W(z) \end{Bmatrix} \tag{3.3}$$

Where, ω is the frequency of steady state vibration and $H_j^{(2)}$ is Hankel function of the second kind of order j,

Substituting the potential functions in 1 and 2 yields,

$$\alpha^2(\lambda + 2G)\phi - G\frac{d^2\phi}{dz} + \alpha(\lambda + G)\frac{dW}{dz} - \rho\omega^2\phi = 0 \tag{3.4}$$

$$-\alpha(\lambda + G)\frac{d\phi}{dz} + \alpha^2 GW - (\lambda + 2G)\frac{d^2W}{dz^2} - \rho\omega^2 W = 0 \tag{3.5}$$

Now, the stresses between the layer soil element boundary are given by,

$$\sigma_{zr} = G\left(\frac{\partial v_r}{\partial z} + \frac{\partial v_z}{\partial r}\right)$$
$$\sigma_{zz} = \lambda\left(\frac{1}{r}\frac{\partial}{\partial r}(rv_r + \frac{\partial v_z}{\partial z})\right) + 2G\frac{\partial v_z}{\partial z}$$

The stresses can be expressed as,

$$\begin{Bmatrix}\sigma_{zr}\\ \sigma_{zz}\end{Bmatrix} = \begin{bmatrix} H_1^{(2)}(\alpha r) & 0 \\ 0 & H_0^{(2)}(\alpha r)\end{bmatrix}\begin{Bmatrix}\overline{\sigma_1}\\ \overline{\sigma_2}\end{Bmatrix} \tag{3.6}$$

Where,
$\overline{\sigma_1} = G\left[\frac{d\phi}{dz} - \alpha W\right], \overline{\sigma_2} = \alpha\lambda\phi + (\lambda + 2G)\frac{dW}{dz}$

since the transformation matrix between $v_r, v_z \text{ and } \phi, W$ (Equation 3.3) and that between σ_{zr}, σ_{zz} and $\overline{\sigma_1}, \overline{\sigma_2}$ (Equation 3.6) is same, Galarkin method can be applied for equations 3.4 and 3.5 with stress terms as $\overline{\sigma_1}, \overline{\sigma_2}$

Applying Galarkin's Method yields the following equations of motion for each two node layer element with liner shape function.

$$\left(\alpha^2\left[A_p\right]^c + [G_s]^c - \omega^2[M]^c\right)\{\phi\}^c - \alpha([B]^c)\{W\}^c = \{\overline{\sigma_1}\} \tag{3.7}$$

$$-\alpha[B]^c\{\phi\}^c + (\alpha^2[A_s]^c + [G_p\}^c - \omega^2[M]^c\{W\}^c = \{\overline{\sigma_2}\} \tag{3.8}$$

Where,

$$[A_s]^c = GH\frac{1}{6}\begin{bmatrix}2 & 1\\ 1 & 2\end{bmatrix}, [G_s]^c = \frac{G}{H}\begin{bmatrix}1 & -1\\ -1 & 1\end{bmatrix}$$

$$[A_p]^c = (\lambda + 2G)\frac{H}{6}\begin{bmatrix}2 & 1\\ 1 & 2\end{bmatrix}, [G_p]^c = \frac{\lambda + 2G}{H}\begin{bmatrix}1 & -1\\ -1 & 1\end{bmatrix}$$

$$[B]^c = \begin{bmatrix}\frac{\lambda - G}{2} & \frac{\lambda + G}{2}\\ -\frac{\lambda + G}{2} & -\frac{\lambda - G}{2}\end{bmatrix}, [M]^c = \rho H\frac{1}{6}\begin{bmatrix}2 & 1\\ 1 & 2\end{bmatrix}$$

In which H is the thickness of a layer element.

Assembling the global matrices, one gets

$$(\alpha^2[A_p]+[G_s]-\omega^2[M])\{\phi\}-\alpha[B]^T\{W\}=0$$

$$-\alpha[B]\omega^2+(\alpha^2[A_s]+[G_p]-\omega^2[M])\{W\}=0$$

Tajimi and Shimomura [11] derived exactly similar equations for their transformed displacements in lateral vibration. Hence there is a direct analytical correspondence between transformed displacements of zonal and lateral vibrations. The above equations are solved in the manner of an exigent-value problem. There exist a total of 4N solutions of a. Imposing radiation condition, the number of appropriate eigen-values will be 2 N.

A foundation with a circular cross-section is assumed to be obtained on the wall of the cylindrical hollow. The boundary displacement components in radial and vertical direction are respectively expressed as,

$$\{V_r\}=\frac{\sum}{a}H_1^{(2)}(\alpha r0)\{\phi)_a q_\alpha$$

$$\{V_z\}=\frac{\sum}{a}H_0^{(2)}(\alpha r_0)\{W)_a q_\alpha$$

where q_α is the effective contribution corresponding to a.

Modal matrices can be defined as,

$$[X] = [\{\phi\}_1\{\phi\}_2 \ldots \{\phi\}_{2N}]$$

$$[Z] = [\{W\}_1\{W\}_2 \ldots \{W\}_{2N}]$$

Now,

$$\begin{bmatrix}\{V_r\}\\ \{V_z\}\end{bmatrix}=[[Z]\begin{bmatrix}[X] & & \\ & g_\alpha & \\ & & \ddots\end{bmatrix}\{\{\bar{q}_\alpha\}=[J_z]\{\bar{q}_\alpha\} \qquad (3.9)$$

Where, $\bar{q}_\alpha = q_\alpha H_1^{(2)}(\alpha r_o) and g_\alpha = \frac{H_9^{(2)}(\alpha r_0)}{H_1^{(2)}(\alpha r_0)}$.

The vertical stress on the boundary of hollow cylinder is given by,

$$\sigma_{rz} = -G\left(\frac{\partial v_r}{\partial_z} + \frac{\partial v_z}{\partial_r}\right)_{r=r_o}$$

Integrating the stress over the whole circumference would give,

$$P_z = 2\pi r_o \sigma_{rz}\Big|_{r=r_o}$$

The nodal forces can be obtained as,

$$\frac{1}{2\pi r_o}\{P_z\}^c = \frac{G}{2}\begin{bmatrix}1 & -1\\ 1 & -1\end{bmatrix}\begin{Bmatrix}\phi_1\\ \phi_2\end{Bmatrix}H_1^{(2)}(\alpha r_o) + \alpha\frac{GH}{6}\begin{bmatrix}2 & 1\\ 1 & 2\end{bmatrix}\begin{Bmatrix}W_1\\ W_2\end{Bmatrix}H_1^{(2)}(\alpha r_o)$$

The global force vector can be expressed as,

$$\frac{1}{2\pi r_o}\{P_{z_s}\} = \left[[B_G]^T[X] + [A_s][Z]\begin{bmatrix}\ddots & & \\ & \alpha & \\ & & \ddots\end{bmatrix}\right]\{\bar{q}_\alpha\} = [D_z]\{\bar{q}_o\} \qquad (3.10)$$

Where,

$$[B_G]^c = \frac{G}{2}\begin{bmatrix}1 & 1\\ -1 & -1\end{bmatrix}$$

From 9 and 10,

$$\{P_{z_s}\} = [R_z]\begin{Bmatrix}\{V_r\}\\ \{V_z\}\end{Bmatrix} = [R_{z1} \vdots R_{z2}]\begin{Bmatrix}\{V_r\}\\ \{V_z\}\end{Bmatrix}$$

Where, $[R_z] = 2\pi r_0[D_z][J_z]^{-1}$.

Ignoring the coupling with V_r ,

$$\{P_{z_s}\} = [R_{z2}]\{V_z\} \qquad (3.11)$$

The pile force-displacement relationship can be expressed as,

$\{P_{z_p}\} = [K]\ \{w\}$

where the pile axial stiffness matrix,

$$[K] = \begin{pmatrix} \frac{AE}{h_1} & -\frac{AE}{h_1} & & & \\ -\frac{AE}{h_1} & \frac{AE}{h_1}+\frac{AE}{h_2} & & & \\ & \frac{AE}{h_2}+\frac{AE}{h_3} & -\frac{AE}{h_3} & & \\ & & \ddots & & \\ & & & -\frac{AE}{h_{n-1}} & \frac{AE}{h_{n-1}}+\frac{AE}{h_n} \end{pmatrix}$$

The equation of mition will then be given by,

$$([K]-\omega^2[M_z])\{w\} = \{p_{z_p}\} \qquad (3.12)$$

Where $[M_z]$ is the pile mass matrix.

Considering compatibility, from 3.11 and 3.12 we get,

$$([R_{z2}]+[K]-\omega^2[M_z])\{V_z\} = \{P_z\}$$

3.2 Simplified expression of pile head axial stiffness

In order to study the interaction between the superstructure and the substructure of embedded pile, the solution of the present method must be combined with the model of superstructure. Usually this done by the Method of Sub structuring, where the superstructure is modeled numerically or a physical model of superstructure is tested and the effect of substructure is introduced with some impedance function. In most of the applications this impedance function is preferred to be as possible.

This is particularly true for experiments the superstructure is physically modeled and the effect of substructure is simulated in real time with a transfer function.

In order to derive a simplified expression of pile head axial stiffness. let us first consider the equation of vertical motion ω (r, z, t) of an elastic medium neglecting the horizontal displacement.

$$(\lambda + 2\mu)\frac{\partial^2 \omega}{\partial z^2} + \mu\left(\frac{1}{r}\frac{\partial}{\partial r} + \frac{\partial^2}{\partial r^2}\right)\omega = \rho\frac{\partial^2 \omega}{\partial t^2} \tag{3.13}$$

Now, Konagai et.al. (2000) Proposed that in lateral vibration the pile deforms only down to some active pile length which is closely related to the following parameter L_{0l} :

$$L_{0l} = \sqrt[4]{\frac{EI}{\mu}}$$

where EI is the bending stiffness of pile and μ is the shear modulus of soil.

Analogously, for axial vibration here the relative pile stiffness to soil stiffness is represented by a length parameter L_{0a}:

$$L_{0a} = \sqrt{\frac{AE}{\mu}} \tag{3.14}$$

where AE is the axial stiffness of pile. Then the active length for axial vibration may be given as:

$$L_{aa} = a_0 L_{0a} \tag{3.15}$$

Now, assuming the axial deformation of pile occurs within the active pile length, the Independent variables of vertical deformation may be separated as:

$$\omega = \sum_{i=1}^{\infty} W(r)\varphi_i\left(\frac{z}{L_{aa}}\right)e^{iwt} \tag{3.16}$$

where, φ_i represents a mode shape.

Substituting ω in Equation. 3.13 with the expression of Equation 3.16.

$$\sum_{i=1}^{\infty}(\lambda+2\mu)We^{iwt}\frac{\partial^2\varphi i}{\partial z^2}+\sum_{i=1}^{\infty}\mu\varphi_i e^{iwt}\left(\frac{1}{r}\frac{\partial}{\partial r}+\frac{\partial^2}{\partial r^2}\right)W=\sum_{i=1}^{\infty}-\rho\omega^2W\varphi_i e^{iwt}$$

Multiplying with φ_n and integrating over the whole depth of active length,

$$\sum_{i=1}^{\infty}W\int_o^{Laa}(\lambda+2\mu)\varphi_n\frac{\partial^2\varphi_n}{\partial_{z^2}}dz+\sum_{i=1}^{\infty}(\frac{1}{r}\frac{\partial}{\partial r}+\frac{\partial^2}{\partial_{r^2}})W\int_o^{Laa}\mu\phi_n\phi_i dz=\sum_{i=1}^{\infty}-\omega^2W\int_o^{Laa}\rho\varphi_n\varphi_n dz$$

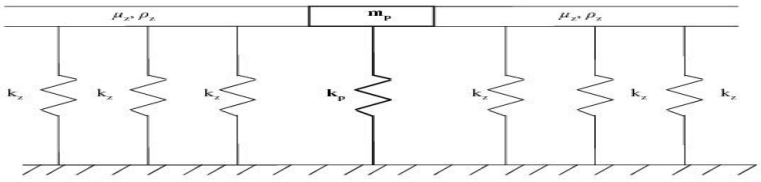

Figure 3.2: Infinite soil –extent in plane strain condition supported by Winkler type springs with embedded pile

Considering orthogonally of mode shapes one obtains,

$$W\int_o^{Laa}(\lambda+2\mu)\varphi_n\frac{\partial^2\varphi_n}{\partial_{z^2}}dz+(\frac{1}{r}\frac{\partial}{\partial r}+\frac{\partial^2}{\partial_{r^2}})W\int_o^{Laa}\varphi\mu_n\mu_n dz=-\omega^2W\int_o^{Laa}\rho\varphi_n\varphi_n dz$$

Expressing

$\int_o^{Laa}\mu\varphi^2{}_n dz=\mu_z and\int_o^{Laa}\rho\varphi^2{}_n dz=\rho_z onegets,$

$$W\int_o^{Laa}(\lambda+2\mu)\varphi_n\frac{\partial^2\varphi_n}{\partial z^2}dz+\varphi_z\left(\frac{1}{r}\frac{\partial}{\partial_r}+\frac{\partial^2}{\partial r^2}W\right)=-\omega^2\rho_z W$$

Integrating the first term of the above equation by parts and assuming the bottom end of the soil pile assemblage as fixed and the top as free from stresses one can write,

$$-W\int_o^{Laa}(\lambda+2\mu)\varphi_n\left(\frac{\partial^2\varphi_n}{\partial z}\right)^2dz+\varphi_z\left(\frac{1}{r}\frac{\partial}{\partial_r}+\frac{\partial^2}{\partial r^2}W\right)=-\omega^2\rho_z W \qquad (3.17)$$

The governing equation of a plane strain formulation with an embedded disk in vertical vibration is given by,

$$\mu_2\left(\frac{1}{2}\frac{d}{dr}+\frac{d^2}{dr^2}\right)W=-\omega^2\rho_z W \qquad (3.18)$$

It can be observed that the first term of Equation. 3.17 is a term additional to the plane strain formulation of Equation. 18. This term represents additional stiffness to the system. Let $\int_o^{Laa}(\lambda+2\mu)\left(\frac{\partial\varphi_n}{\partial z}\right)^2dz=k_z$ them from Equation. 3.17 one can obtain.

$$-k_z W+\mu_z\left(\frac{1}{r}\frac{d}{dr}+\frac{d^2}{dr^2}\right)W=-\omega^2\rho_z W \qquad (3.19)$$

Thus an axi-symmetric formulation can be modeled as an infinite soil extent in plane strain condition supported by Winkler type springs (Figure 3.2).

Let us introduce $\omega_o = \sqrt{\frac{k_z}{\rho_z}}$, Then from Equation. 3.19 one obtains,

$$\mu_z\left(\frac{1}{r}\frac{d}{dr}+\frac{d^r}{dr^2}\right)W = -(\omega^2-\omega_0^2)\rho_z W$$

Introducing $\xi = \sqrt{1-(\frac{\omega_0}{\omega})^2}$,

$$\mu_z\left(\frac{1}{r}\frac{d}{dr}+\frac{d^2}{dr^2}\right)W = -(\omega\xi)^2\rho_z W \qquad (3.20)$$

Comparing Equations 3.18 and 3.20, it is evident that the solution of Equation. 3.20 will be similar to the solution of Equation. 3.18. According to Novak et.al. (1978) the expression of soil stiffness derived from Equation.3.18.is given by,

$$k_\omega = 2\pi\mu_z a_0 \frac{K_1(a_0)}{K_0(a_0)}$$

Where $a_0 = \frac{i\omega r_0}{V_s}$ and $V_s = \sqrt{\frac{\mu_z}{\rho_z}}$

Hence the expression of stiffness for soil as derived from Equation. 3.20 would be,

$$k_\omega^{'} = 2\pi\mu_z a_0^{'} \frac{K_1(a_0^{'})}{K_0(a_0^{'})}$$

where, $a_0^{'} = \frac{i\omega\xi r_0}{V_s}$

The function $\frac{K_1(a_0^{'})}{K_0(a_0^{'})}$ is approximated by $(1+0.4/a_0^{'})$ when the absolute value of $a_0^{'}$ is larger than 0.01 (1998). This simplification leads to

$$k_\omega^{'} = 2\pi\mu_z a_0^{'}(1+0.4/a_0^{'}) \qquad (3.21)$$

Now let us take two limiting cases $\omega \to 0$ and $\omega \to \infty$ For the static case (i.e, $\omega \to 0$), $i\omega\xi \to \omega_0$ and $a_0^{'} \to \frac{\omega_0 r_0}{V_s} = \sqrt{\frac{k_z}{\mu_z}} r_0$

For a homogeneous soil profile one can write $\mu_z = \mu\alpha_1 L_{aa}$ and $k_z = \mu\gamma(\upsilon)\alpha_2/L_{aa}$

where $\alpha_1 = \int_0^1 (\varphi_n(\zeta))^2 d\zeta$, $\alpha_2 = \int_0^1 \left(\frac{d\varphi_n(\zeta)}{d\zeta}\right)^2 d\zeta$, $\gamma(\upsilon) = \frac{2(1-\upsilon)}{1-2\upsilon}$

where α_3 is a function of the deformed shape and Poisson's ratio.

$$a_0' - \sqrt{\gamma \frac{\alpha_1}{\alpha_2}} \frac{r_0}{L_{aa}} = \alpha_3 \frac{r_0}{L_{aa}}$$

From Equation. 3.21,

$$k_\omega' \approx 2\pi\alpha_1 \mu L_{aa} \left(\alpha_3 \frac{r_0}{L_{aa}} + 0.4\right) = \left(2\pi\alpha_1\alpha_3 \frac{r_0}{L_{aa}} + 0.8\pi\alpha_1\right) \quad (3.22)$$

For the dynamic case $\omega \to \infty$ and $\xi \to 1$ Thus,

$$a_0' = \frac{i\omega r_0}{V_s} = \mathrm{i}\, a$$

From Equation .3.21,

$$k_\omega' = \mu L_{aa} (i2\pi\alpha_1 a \;\; 0.8\pi a) \quad (3.23)$$

Considering soil as a visco-elastic medium, from Equations 3.22 and 3.23 soil stiffness may be approximated as,

$$k_\omega' \approx \mu L_{aa} \left\{\left(2\pi\alpha_1\alpha_3 \frac{r_0}{L_{aa}} + 0.8\pi\alpha_1\right) + i2\pi\alpha_1 a\right\} \quad (3.24)$$

The stiffness of the pile itself is given by,

$$k_p \quad - \quad \alpha_2 \frac{AE}{L_{aa}}$$

From Equations 3.14 and 3.15 the stiffness can be expressed as,

$$k_p = \frac{c_2}{c_0^2} \mu L_{aa} \quad (3.25)$$

The contribution of the pile mass to the stiffness is given by,

$$m_p = \int_0^{L_{aa}} \rho_p \pi r_0^2 \varphi_n^2 dz = \bar{\rho}\rho\alpha_1 \pi r_0^2 L_{aa} = \bar{\rho}\alpha_1 \pi \frac{r_0^2}{V_s^2} \mu L_{aa} \quad (3.26)$$

where. $p = \frac{p_r}{p}$,

Then the overall stiffness K_{zz} of the pile cap for vertical motion can be written as,

$$K_{zz} = K_{\omega}^{'} + K_p - m_p\omega^2 \tag{3.27}$$

Using Equations 3.24, 3.25 and 3.26, equation.3.27 can be written as:

$$K_{zz} \approx \mu L_{aa}\left\{\left(2\pi\alpha_1\alpha_3\frac{r_0}{L_{aa}} + 0.8\pi\alpha_1 + \frac{\alpha_2}{\frac{2}{\alpha_0}}\right) + i2\pi\alpha_1 p\alpha^2\right\}$$

Substituting L_{0a} in place of L_{aa} using Equation.3.14.

$$K_{zz} \approx \mu L_{0a}\left\{\left(2\pi\alpha_1\alpha_3\frac{r_0}{L_{aa}} + 0.8\pi_0\alpha_1 + \frac{\alpha_2}{\alpha_0}\right) + i2\pi\alpha_0\alpha_1\rho\alpha^2\right\} \tag{3.28}$$

Hence the system can be modeled as a simple oscillator,

$$K_{zz} \approx K_0 + ic_0\alpha - m_0\alpha^2 \tag{3.29}$$

$$\frac{K_0}{\mu L_{0a}} = c_1\frac{r_0}{L0_a} + c_2, \frac{c_0}{\mu L_{0a}} = c_4\overline{\rho}$$

and ,

$$c_1 = 2\pi\alpha_1\alpha_3, c_2 = 0.8\pi\alpha_0\alpha_1 + \frac{\alpha_2}{\alpha_0}, c_3 = c_3 2\pi\alpha_0\alpha_1 and c_4 = \pi\alpha_0\alpha_1$$

Here the parameters c_1, c_2, c_3 and c_4 basically depend on the predominant mode φ_n of axial pile deformation and the relation between the parameter L_{0a}, and the active pile length for axial vibration (Equation.3.15). In addition $C_3$and as such C_1 depends on Poisson's ratio too.

In addition to the parameters μ and L_{oa}, the stiffness term k_0 depends on r_0 and υ and mass term depends on $\bar{\rho}$. In the derivation of Equation. 3.29 many simplifications have been adopted. Hence the applicability of the equation has been checked by comparing it with the results obtained from more rigorous solution of TLEM. The parameters c_1, c_2, c_3, and c_4 are then obtained in such a way that the overall error is minimized for the variety of soil and pile parameters. The parameters that have been considered are pile parameters such as radius, length and modulus of elasticity and soil parameters such as shear modulus, Poisson's ratio and damping ratio. In this discussion only a homogeneous soil profile and solid cross-section of pile is considered. The best fit of the values from Equation. 3.29. to rigorous solution of k_{zz} is obtained by setting c_1, c_2, c_3, and c_4 at π, 2π/5, 2π/3 and π/300 respectively.

The material damping of soil may be considered in the simple expression of k_{zz} by replacing shear modulus μ with complex modulus $\dot{\mu}$ (1+ i D). Introduction of complex modulus however causes the stiffness and damping parameters k_0 and c_0 in Equation.

$$\frac{k_0}{\mu' L_{0a}} = \left(\pi \frac{r_0}{L_{0a}} + \frac{2\pi}{5}\right) - \frac{2\pi}{3} D_{\mu} \qquad (3.30)$$

$$\frac{c_0}{\mu' L_{0a}} = \frac{2\pi}{3}\left(\pi \frac{r_0}{L_{0a}} + \frac{2\pi}{5} - \frac{\pi}{300}\alpha^2\right) D \qquad (3.31)$$

When the effect of D cannot be ignored in Equation. 3.30 and 3.31 the most predominant frequency a should be used in calculating k_0 and c_0.

3.3 Modal Analysis of a pier with batter piles

Axial pile head stiffness plays an important role for batter piles even for horizontal vibration. Batter piles are usually inclined at an angle of 10° or a slope 11H: 6V. For such mild slope, pile head stiffness of a single batter pile may not differ significantly from that of a vertical pile. However the orientation of t he axial and lateral stiffness of a batter pile is inclined by the batter angle. Thus as show in Figure 3.3 the substructure (i,e, the pile cap along with the pole-soil system) may be modeled with axial and lateral springs substituted for the piles aus soil, if pile-to pile interaction can be ignored. Usually pile to pile interaction becomes important for very high frequency. Then pile cap stiffness may be expressed in terms of axial and vertical spring stiffness and the batter angle.

$$\begin{Bmatrix} F_{z,cap} \\ F_{x,cap} \\ M_{cap} \end{Bmatrix} = [K_{cap}] \begin{Bmatrix} u_z \\ u_x \\ \emptyset \end{Bmatrix}$$

Where,

$$K_{cap1,1} = \sum_i K_{x,i} \sin^2\theta_i + k_{z,i} \cos^2\theta_i$$

$$K_{cap1,2} = K_{cap2,1} = \sum_i (K_{x,i} - k_{z,i}) \sin\theta_i \cos\theta_i$$

$$K_{cap1,3} = K_{cap3,1} = \sum_i x_i (K_{x,i} \sin^2\theta_i + k_{z,i} \cos^2\theta_i)$$

$$K_{cap2,2} = \sum_i K_{x,i} \cos^2\theta_i + k_{z,i} \sin^2\theta_i$$

$$K_{cap2,3} = K_{cap3,2} = \sum_i x_i (K_{x,i} - k_{z,i}) \sin\theta_i \cos\theta_i$$

$$K_{cap3,3} = \sum_i x_i^2 (K_{x,i} \sin^2\theta_i + K_{x,i} \cos^2\theta_i)$$

The superstructure is modeled as a single mass supported by a Bernoulli- Euler beam. The stiffness equation for the superstructure may be written as,

$$\begin{Bmatrix} F_{z,1} \\ F_{x,1} \\ M_1 \\ F_{z,2} \\ F_{x,2} \\ M_2 \end{Bmatrix} = \begin{bmatrix} \frac{EA}{L} & 0 & 0 & -\frac{EA}{L} & 0 & 0 \\ 0 & \frac{12EI}{L^3} & \frac{6EI}{L^2} & 0 & -\frac{12EI}{L^3} & \frac{6EI}{L^2} \\ 0 & \frac{6EI}{L^2} & \frac{4EI}{L} & 0 & -\frac{6EI}{L^2} & \frac{2EI}{L} \\ -\frac{EA}{L} & 0 & 0 & \frac{EA}{L} & 0 & 0 \\ 0 & \frac{12EI}{L^3} & \frac{6EI}{L^2} & 0 & \frac{12EI}{L^3} & \frac{6EI}{L^2} \\ 0 & \frac{6EI}{L^2} & \frac{2EI}{L} & 0 & -\frac{6EI}{L^2} & \frac{4EI}{L} \end{bmatrix} \begin{Bmatrix} u_{z,1} \\ u_{x,1} \\ \phi_1 \\ u_{z,2} \\ u_{x,2} \\ \phi_1 \end{Bmatrix}$$

$$= \begin{bmatrix} K_{col1,1} & K_{col1,2} \\ K_{col2,1} & K_{col2,2} \end{bmatrix} \begin{Bmatrix} u_1 \\ u_2 \end{Bmatrix} \qquad (3.32)$$

If the mass terms corresponding to the degrees of freedom of Equation 3.32 are represented by the vector $\{m_{x,1}\ m_{x,1}\ \emptyset_1\ m_{x,2}\ m_{x,2}\ \emptyset_2\}^T = \{m_1\ m_2\}$, the homogenous equation of motion for the combined pier –pile system can be expressed as:

$$\begin{bmatrix} m_1 & 0 \\ 0 & m_2 \end{bmatrix} \begin{Bmatrix} \ddot{u}_1 \\ \ddot{u}_2 \end{Bmatrix} + \begin{bmatrix} K_{col1,1} & K_{col1,2} \\ K_{col2,1} & K_{col2,2} + K_{cap} \end{bmatrix} \begin{Bmatrix} u_1 \\ u_2 \end{Bmatrix} = \begin{Bmatrix} 0 \\ 0 \end{Bmatrix}$$

$$\begin{bmatrix} K_{col1,1} - m_1\omega^2 & K_{col1,2} \\ K_{col2,1} & K_{col2,2} + K_{cap} - m_2\omega^2 \end{bmatrix} \begin{Bmatrix} u_1 \\ u_2 \end{Bmatrix} = \begin{Bmatrix} 0 \\ 0 \end{Bmatrix} \quad (3.33)$$

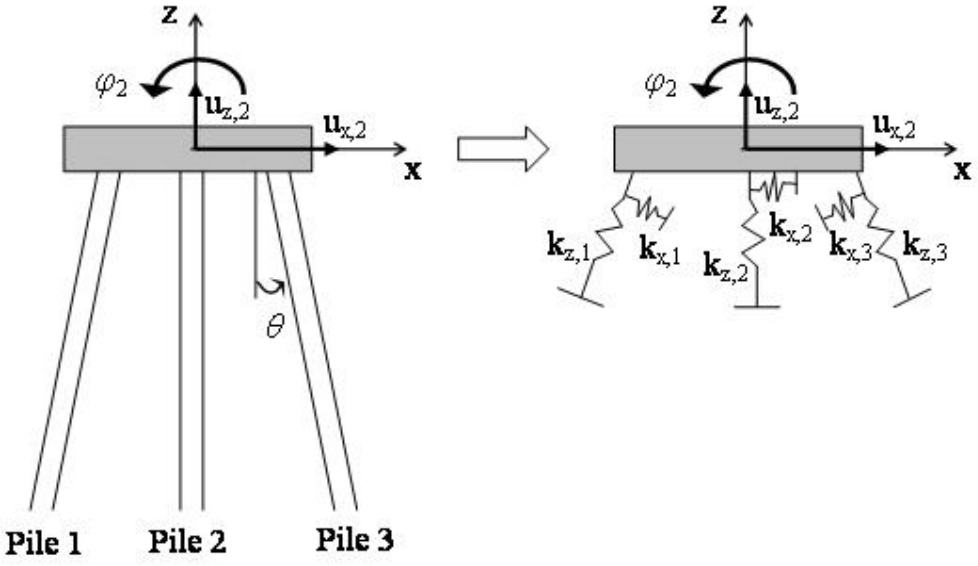

Figure 3.3 : Simple spring model of piles

The solution of the eigen-value problem of Equation 3.33 would yield the eigen frequencies and corresponding normal modal vectors of the system.

3.4 Kinematic interaction

Instead of solving the eigen-value problem expressed by Equation. 3.33. forces that would be produced at the pile cap due to deformation of soil may be applied. Thus the following non-homogeneous equation may be solved in frequency domain.

$$\begin{bmatrix} K_{col1,1} - m_1\omega^2 & K_{col1,2} \\ K_{col2,1} & K_{col2,2} + K_{cap} - m_2\omega^2 \end{bmatrix} \begin{Bmatrix} u_1 \\ u_2 \end{Bmatrix} = \begin{Bmatrix} 0 \\ F_{cap} \end{Bmatrix} \quad (3.34)$$

However, the inability of an embedded pile foundation to conform to the deformation of soil causes the motion of the soil structure interface to deviate from the free-field motion u_f. The foundation input motion should be modified to incorporate this deviation (u_s) due to the kinematic interaction. The foundation input motion for the Yanagizawa bridge piers is estimated rigorously by the Thin Layered Element Method (1976). The kinematic interaction factors, $T_e = \frac{u_f + u_x}{u_f}$ for motions in different directions. Thus without the presence of a superstructure, a horizontal free-field motion of $u_{f,x}$. would cause a horizontal displacement of $T_{e,x}$, $u_{f,x}$ and a rotation of $T_{e,\phi x}$,$u_{f,x}$ of

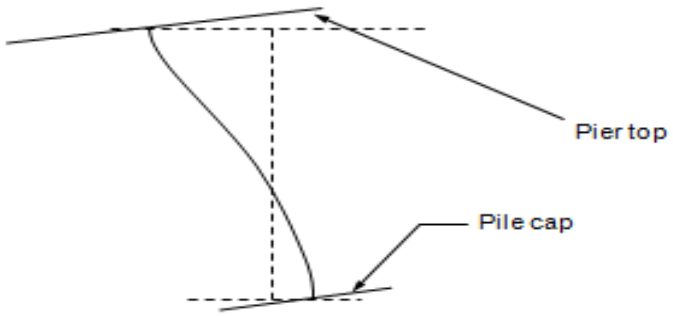

Figure 3.4: First mode of vibration for higher batter angles

the pile head producing the following forces at the pole head:

$$f_{p,1}^{i} = \begin{bmatrix} (k_x^i - k_z^i)sin0^i\,cos0^i & 0 \\ k_z^i sin^2 0^i + k_x^i cos^2 0^i & k_{\emptyset x}^i\,cos0^i \\ k_{\emptyset x}^i\,cos0^i & k_{\emptyset}^i \end{bmatrix} \begin{Bmatrix} T_{e,x}^i \\ T_{e,\emptyset x}^i \end{Bmatrix} \quad (3.35)$$

In case of a vertical free-field motion of $u_{f,z}$, the pile head would experience a vertical displacement of $T_{e,z}$, $u_{f,z}$ and the forces on the pile head would be:

$$f_{p,1}^{i} = u_{f,z} T_{e,z}^{i} \begin{Bmatrix} k_z^i cos^2 0^i + k_x^i sin^2 0^i \\ (k_x^i - k_z^i)sin0^i\,cos0^i \\ k_{\emptyset x}^i\,sin0^i \end{Bmatrix} \quad (3.36)$$

In either case, the forces on the pile cap, including the additional moment due to the vertical force at each pile head, would be:

$$F_{cap} = \sum_i f_{p,i}^{i} + \begin{Bmatrix} 0 \\ 0 \\ \sum_i x^i f_{p,1,1}^{i} \end{Bmatrix} \quad (3.37)$$

Now solving Equation 3.35 with forces from equation 3.37 will provide displacements and rotations of pier top and pile cap considering both inertial and kinematic interaction at a particular excitation frequency.

3.5 Parameter of the Present Study

The pile head stiffness will be determined by the Thin Layered Element Method (TLEM) considering semi-infinite layered soil profile. The substructure i,e. the pile cap along with the pile soil system will be considered such as pile to pile interaction will be ignored. The individual pile stiffness will be considered as complex stiffness. Only stiffness and damping properties will be considered from the substructure.

Modal analysis of a viaduct-pile system will be conducted by Mathmatica 5.0 and the kinematic interaction between a viaduct and the pile foundation will be investigated by sub-structure method.

CHAPTER 4

RESULTS AND DISCUSSIONS

In this chapter it has been discussed the findings of the present study which are summarized as follows:

i) In the previous study it has been shown that for a certain batter angle between 15 ° and 20° the pile cap deformation in the first mode of vibration becomes zero. Beyond this particular batter angle the pile cap deformation again increases and actually becomes out –of- phase with the pier top deformation. From fig 4.1 it can be observed that for low batter angle pier top deformation are in phase and pier top rotation & pile top rotation are out-of-phase. That means a right ward pier top deformation and clockwise pier top & anti-clockwise pile top rotations occur at low batter angles. Fig 4.1 also shows that for greater batter angles, the pier top deformation is out of phase and rotations are in phase and anti-clockwise rotations at both pier top and pile cap occur. It also observed that phase are changed at 17° batter angle.

ii) Modal behavior of pier top deformation, pier top rotation & pile top rotation has also been observed by considering half of the pier length where other data remain unchanged (fig. 4.2). From this fig. it can be observed that for low batter angle pier top deformation are also in phase and pier top rotation & pile top rotation are also out-of-phase. But a certain batter angle between 10 ° and 15° the phases are changed.

ii) Fig. 4.3 shows that in lower frequencies pier goes through almost rigid body motion. Frequency greater than 3.5 Hz, pier top deformations increase. But the rate of change of pier top deformation increases with the increase of batter angle. The fig.

also shows that in lower frequencies pier top deformation are out of phase and in higher frequencies the same are in phase.

iii) Fig. 4.4 shows that resonance frequency occurs at frequency of 2.4 Hz. There have no significant effect of batter angle on phase difference between pier top and pile cap rotation.

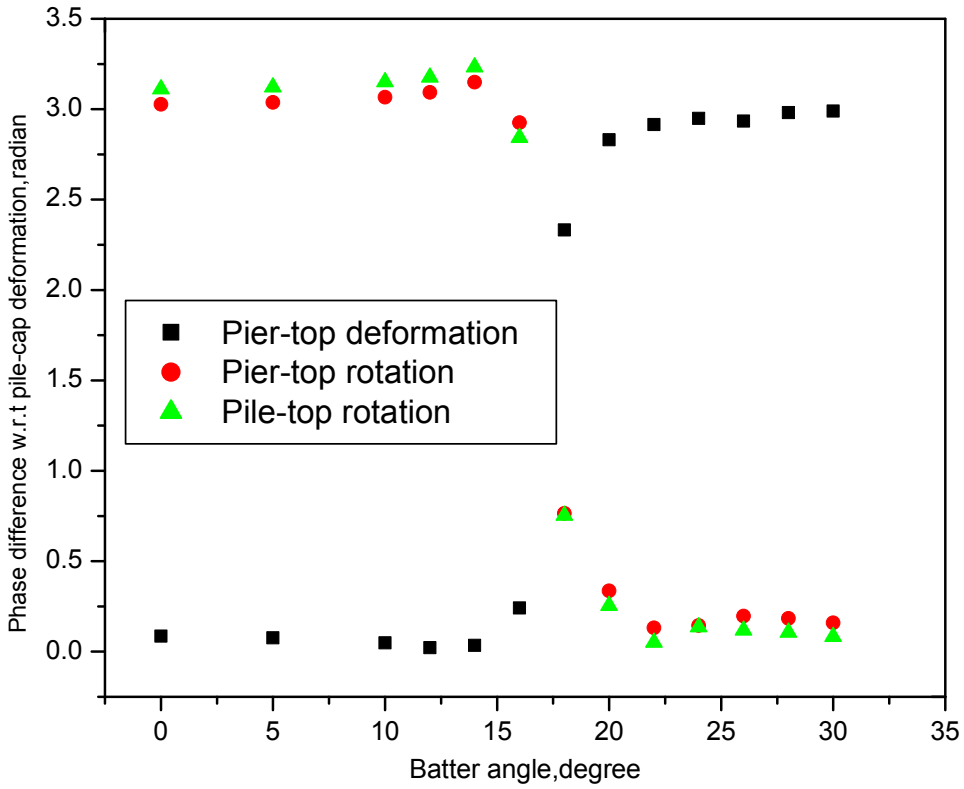

Figure 4.1: Phase difference of modal deformations w, r, t pile cap deformations in radian at various Batter angle where pier length 12.5 m

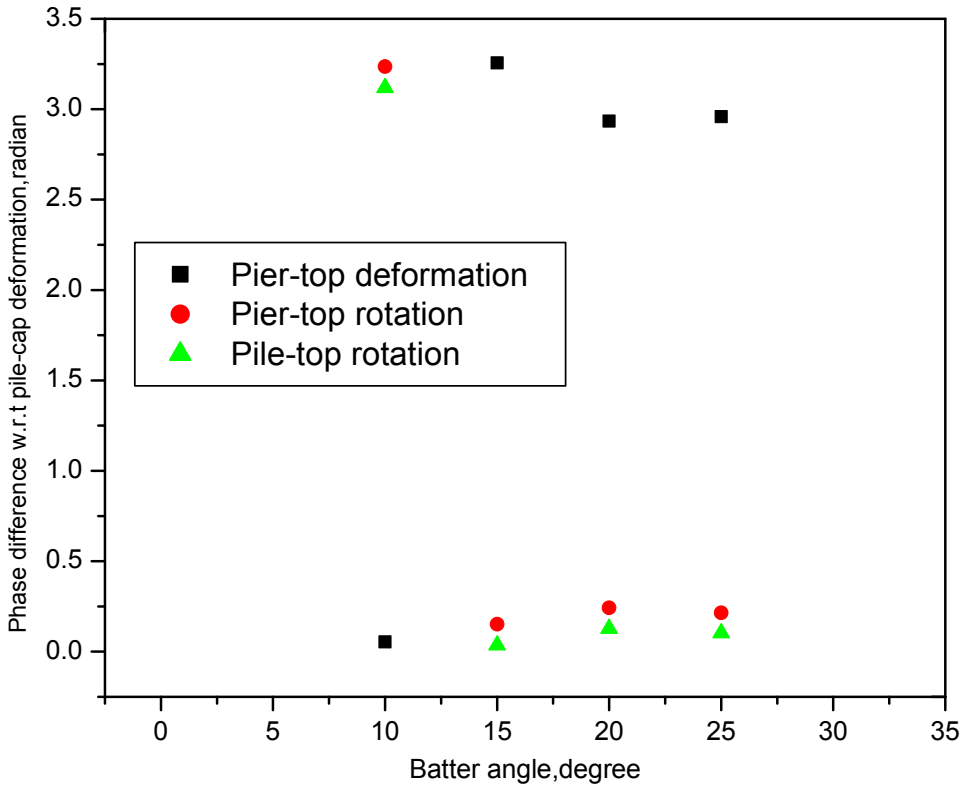

Figure 4.2: Phase difference of modal deformations w, r, t pile cap deformations in radian at various Batter angles considering 6 m pier length

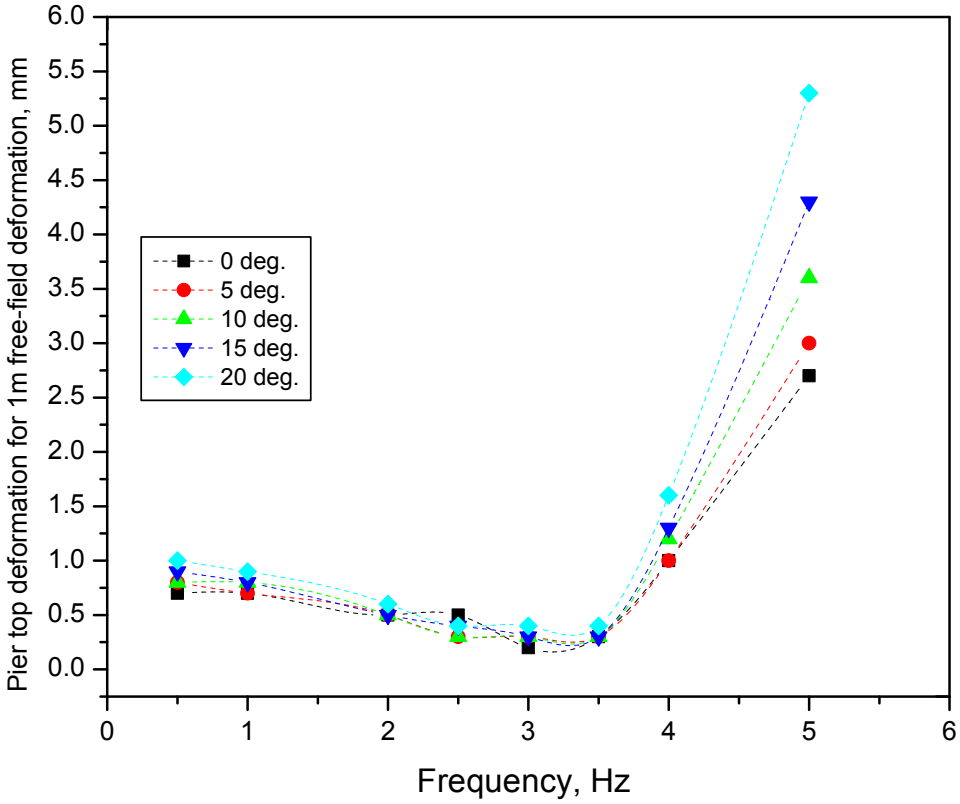

Figure 4.3: Pier top deformations for 1 m free field deformations in mm at different Batter angle at different frequencies.

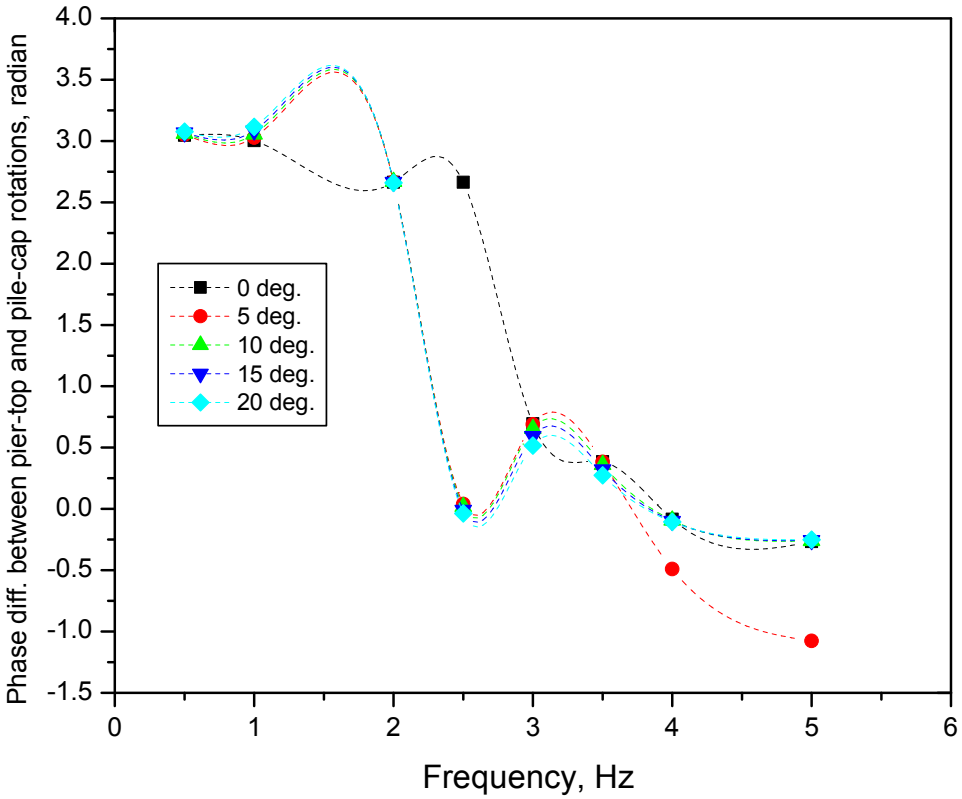

Figure 4.4: Phase difference between pier top and pile cap deformations w, r, t various frequencies in radians at different Batter angle.

CHAPTER 5
CONCLUSIONS AND RECOMMENDATIONS

5.1 General

The main objective of the present study is to evaluate modal behaviour of Batter piles at various Batter angles and To evaluate pier top deformations of Batter pile with respect to free field deformations at different batter angle with different frequencies.

The pile head stiffness will be determined by the Thin Layered Element Method (TLEM) considering semi-infinite layered soil profile. The substructure i,e. the pile cap along with the pile soil system will be considered such as pile to pile interaction will be ignored. The individual pile stiffness will be considered as complex stiffness. Only stiffness and damping properties will be considered from the substructure.

Modal analysis of a viaduct-pile system will be conducted by Mathmatica 5.0 and the kinematic interaction between a viaduct and the pile foundation will be investigated by sub-structure method.

5.2 Conclusions

Findings of the study as presented in the previous chapters are summarized bellows:

i) In the present study it has been observed that for low batter angle pier top deformation are in phase and pier top rotation & pile top rotation are out-of-phase. That means a right ward pier top deformation and clockwise pier top & anti-clockwise pile top rotations occur at low batter angles. It has been also observed that for greater batter angles, the pier top deformation is out of phase and rotations are in phase and anti-clockwise rotations at both pier top and pile cap occur.

ii) In the present study it has been observed that in lower frequencies pier goes through almost rigid body motion. Frequency greater than 3.5 Hz, pier top deformations increase. But the rate of change of pier top deformation increases with the increase of batter angle. It has been also observed that in lower frequencies pier top deformation are out of phase and in higher frequencies the same are in phase.

iii) It has been also observed that at resonance frequency there have no significant effect of batter angle on phase difference between pier top and pile cap rotation.

.

5.3 Recommendation

- In the study, same soil conditions were selected. Different type of soil conditions can also be selected.
- In the study, same number pile was selected. Different number of pile can also be selected.
- The results may also be varied due to type of foundations.
- The results may also be varied due to parameter of the structure.

References:

[1] Alimohammad, S., and Mahmood, V., "Dynamic Study of Batter Pile Groups under Seismic Excitations through Finite Element Method.", World Academy of Science, Engineering and Technology 2009,50.

[2] George, G., and George, M., "Seismic soil–structure interaction: new evidence and emerging issues, Geotechnical Earthquake Engineering and Soil Dynamics", Geo-Institute ASCE Conference, Seattle;1998, 3–6 August.

[3] Juran, I., Benslimane, A., and Hanna, S., "Engineering analysis of dynamic behavior of micro pile systems", Transportation Research Record No.1772. Soil Mech 2001;91–106.

[4] Tasaki, T., Katsumi, S., and Toshihiro, W., "Seismic observations and analysis of grouped piles." Shimizu. Technical Research Bulletin,1988, 7:17-32.

[5] Tim, J.I., Santiago, R, Roupen, D., and John, C., "Seismic analysis of bridges with pile foundations". Computers and Structures,1999,72:19.62.

[6] Rajashree, S.S.,and Sitharam, T.G.,"Nonlinear finite-element modeling of batter piles under lateral load. Journal of Geotechnical and Geo-environmental Engineering",July,2001,127(7):604-612.

[7] Ahsan, R., Konagai, K., Johansson, J., and Tanaka, H., "Analysis of Axial vibration of Piles in layered soil media and application to Batter pile foundations, New Technologies for Urban safety of Mega cities in Asia ed: M.H. Ansary and K. Worakanchana, ICUS Report, 2007.

[8] Konagai, K., and Ahsan, R., Simulation of nonlinear soil structure interaction on a shaking table. Journal of Earthquake Engineering, 2002, 6.(1) : 31-51.

[9] Konagai, K., Ahsan, R., and Daiske, M., Simple expression of the dynamic stiffness of grouped Piles in sway motion. Journal of Earthquake Engineering, 2000, 4(3): 355-376.

[10] Tazoh, T., Shimizu, K., and Wakahara, T., Seismic observations and analysis of grouped piles. Shimizu. Technical Research Bulletin, 1988, 7:17-32.

[11] Tajimi, H., and Shimomura, Y., Dynamic analysis of soil structure interaction by the thin layered element method. Transactions of Architecture Institute of Japan, 1976, 243:41-51.

[12] Nogami, T., and Novak, M., Soil-pile interaction in vertical vibration. Earthquake Engineering and Structural Dynamics, 1976, 4:277-293.

[13] Yang, J., and Sato, T., Interpretation of seismic vertical amplification observed at an array site. Bulletin of the Seismological Society of America, 2000, 90(2): 275-285.

APPENDICES

APPENDIX-A

SL. No.	Batter angle	Phase difference w, r, t pile cap deformations in radian at various Batter angle		
		Pier-top deformation	Pier-top rotation	Pile-top rotation
01	0^0	0.086	3.027	3.111
02	5^0	0.076	3.038	3.122
03	10^0	0.048	3.066	3.150
04	12^0	0.022	3.093	3.176
05	14^0	0.034	3.149	3.232
06	16^0	0.241	2.926	2.843
07	18^0	2.332	0.764	0.753
08	20^0	2.831	0.336	0.254
09	22^0	2.915	0.131	0.051
10	24^0	2.949	0.144	0.136
11	26^0	2.934	0.197	0.118
12	28^0	2.981	0.184	0.106
13	30^0	2.990	0.159	0.082

Table 1: Phase difference of modal deformations w, r, t pile cap deformations in radian at various Batter angle

APPENDIX-B

SL. No.	Batter angle	Phase difference w, r, t pile cap deformations in radian at various Batter angle		
		Pier-top deformation	Pier-top rotation	Pile-top rotation
01	10°	0.054	3.236	3.118
02	15°	3.256	0.152	0.036
03	20°	2.934	0.242	0.127
04	25°	2.959	0.215	0.103

Table 2: Phase difference of modal deformations w, r, t pile cap deformations in radian at various Batter angle considering 6m pier length

APPENDIX-C

SL.NO.	Frequency	Pier top deformations for 1 m free field deformations in mm at different Batter angle				
		0^0	5^0	10^0	15^0	20^0
01	0.5	0.7	0.8	0.8	0.9	1.0
02	1.0	0.7	0.7	0.8	0.8	0.9
03	2.0	0.5	0.5	0.5	0.5	0.6
04	2.5	0.5	0.3	0.3	0.4	0.4
05	3.0	0.2	0.3	0.3	0.3	0.4
06	3.5	0.3	0.3	0.3	0.3	0.4
07	4.0	1	1	1.2	1.3	1.6
08	5.0	2.7	3	3.6	4.3	5.3

Table 3: Pier top deformations for 1 m free field deformations in mm at different Batter angle at different frequencies.

APPENDIX-D

SL.NO.	Frequency	Phase difference between pier top and pile cap deformations in radians at different Batter angle				
		0^0	5^0	10^0	15^0	20^0
01	0.5	3.04725	3.053179	3.059921	3.067778	3.076508
02	1.0	3.002284	3.027139	3.054333	3.083841	3.115095
03	2.0	2.663402	2.667318	2.667762	2.665317	2.65973
04	2.5	2.663402	0.040063	0.017757	-0.00925	-0.03737
05	3.0	0.693896	0.690039	0.65354	0.592079	0.516476
06	3.5	0.384611	0.383074	0.360206	0.321444	0.273778
07	4.0	-0.0847	-0.48995	-0.09369	-0.09987	-0.10651
08	5.0	-0.26676	-1.07573	-0.26107	-0.25667	-0.25178

Table 4: Phase differences between pier top and pile cap deformations w, r, t various frequencies in radians at different Batter angle.

APPENDIX-E

Programming by Mathematica 5.0

In this study, pier-top deformation, pier-top rotation and pile-top rotation have been conducted at different Batter angles such as 0^0, 5^0, 10^0, 12^0, 14^0, 16^0, 18^0 and 20^0 using Mathematica 5.0 software. Programming for 10^0 is as follows:

[This is a program to calculate Eigenvalues and Eigenvectors for a dynamic system with non-proportional damping.
This program has been developed for the particular application of a Pier-Pile Model.
The program was developed by Raquib Ahsan on July 12, 2007]

Input Parameters *(The cells with grey boxes need input from the user. There are also two input boxes in the Calculations section)*

Pile Parameters

Pile Positions {Distances from the centroid}

```
x = {-3.6, -3.6, -3.6, -2.6, -2.6,-1.5, -1.5, -1.5, 0, 0, 1.5, 1.5, 1.5, 2.6, 2.6, 3.6,
3.6, 3.6};
```

Batter Angles

```
θ = {-10, -10, -10, -10, -10, -10, -10, -10, 0, 0, 10, 10, 10, 10, 10, 10, 10,
10}*Pi/180;
```

Lateral Stiffness of a single pile (can be a function of frequency)

```
kx=13800+ I 200 ω;
```

Axial Stiffness of a single pile (can be a function of frequency)

```
kz=23200 +I 300 ω;
```

Pier Parameters

Height of the pier

```
l = 12.55;
```

Axial Stiffness

```
ae = 3.6* 2.5 10^6;
```

Lateral Stiffness

```
ei = 12.5*2.5 10^6;
```

Mass Matrix

Mass corresponding to the {vertical comp. of Pier-top, lateral comp of Pier-top, rotation of Pier-top, vertical comp of Pile-cap, lateral comp of Pile-cap, rotation of Pile-cap}

```
m=DiagonalMatrix[{30,30,3000,20,20,1000}];
```

Calculations

Number of Piles

```
n = Length[θ];
```

Pile-Cap Stiffness

```
kcap11=Sum[kx (Sin[θ[[i]]])^2 + kz (Cos[θ[[i]]])^2, {i,1,n}];
kcap12=Sum[(kx  - kz) (Sin[θ[[i]]]) (Cos[θ[[i]]]), {i,1,n}];
kcap13 = Sum[x[[i]] (kx (Sin[θ[[i]]])^2 + kz (Cos[θ[[i]]])^2), {i,1,n}];
kcap21 = kcap12;
```

General :: spell1 : Possible spelling error : new symbol name "kcap21 " is similar to existing symbol "kcap12 ". More...

```
kcap22 = Sum[kx (Cos[θ[[i]]])^2 + kz (Sin[θ[[i]]])^2, {i,1,n}];
kcap23 = Sum[x[[i]] (kx - kz) Sin[θ[[i]]] Cos[θ[[i]]], {i,1,n}];
kcap31 = kcap13;
```

General :: spell1 : Possible spelling error : new symbol name "kcap31 " is similar to existing symbol "kcap13 ". More...

```
kcap32 = kcap23;;
```

General :: spell1 : Possible spelling error : new symbol name "kcap32 " is similar to existing symbol "kcap23 ". More...

```
kcap33 = Sum[(x[[i]])^2 (kx (Sin[θ[[i]]])^2 + kz (Cos[θ[[i]]])^2), {i,1,n}];
kcap= {{kcap11, kcap12, kcap13}, {kcap21, kcap22, kcap23}, {kcap31, kcap32, kcap33}};
MatrixForm[Simplify[N[kcap]]]
```

$$\begin{pmatrix} 413065. + (0. + 5351.75\,i)\,\omega & 0. & -2.0354\times10^{-11} - (0. + 2.63775\times10^{-13}\,i)\,\omega \\ 0. & 252935. + (0. + 3648.25\,i)\,\omega & -65907.3 - (0. + 701.141\,i)\,\omega \\ -2.0354\times10^{-11} - (0. + 2.63775\times10^{-13}\,i)\,\omega & -65907.3 - (0. + 701.141\,i)\,\omega & 2.71103\times10^{6} + (0. + 35133.3\,i)\,\omega \end{pmatrix}$$

Pier Stiffness

```
kcol11 = {{ae/l, 0, 0}, {0, 12 ei/l^3, 6 ei/l^2}, {0, 6 ei/l^2, 4 ei/l}};
kcol12 = {{-ae/l, 0, 0}, {0, -12 ei/l^3, 6 ei/l^2}, {0, -6ei/l^2, 2ei/l}};
kcol21 = {{-ae/l, 0,0}, {0, -12 ei/l^3, -6 ei/l^2}, {0,6ei/l^2, 2 ei/l}};
```

```
General :: spell1 : Possible spelling error : new symbol name "kcol21 " is similar to existing symbol "kcol12 ". More...
kcol22 = {{ae/l, 0, 0}, {0, 12 ei/l^3, -6 ei/l^2}, {0, -6 ei/l^2, 4 ei/l}};
kcol={{kcol11, kcol12}, {kcol21, kcol22}};
MatrixForm[kcol]
```

$$\begin{pmatrix} \begin{pmatrix} 717131. & 0 & 0 \\ 0 & 189714. & 1.19046\times10^{6} \\ 0 & 1.19046\times10^{6} & 9.96016\times10^{6} \end{pmatrix} & \begin{pmatrix} -717131. & 0 & 0 \\ 0 & -189714. & 1.19046\times10^{6} \\ 0 & -1.19046\times10^{6} & 4.98008\times10^{6} \end{pmatrix} \\ \begin{pmatrix} -717131. & 0 & 0 \\ 0 & -189714. & -1.19046\times10^{6} \\ 0 & 1.19046\times10^{6} & 4.98008\times10^{6} \end{pmatrix} & \begin{pmatrix} 717131. & 0 & 0 \\ 0 & 189714. & -1.19046\times10^{6} \\ 0 & -1.19046\times10^{6} & 9.96016\times10^{6} \end{pmatrix} \end{pmatrix}$$

Combined Stiffness

```
k=Array[kij,{6,6}];
Do[kij[i,j]=kcol11[[i,j]],{i,3},{j,3}]
Do[kij[i,j+3]=kcol12[[i,j]],{i,3},{j,3}]
Do[kij[i+3,j]=kcol21[[i,j]],{i,3},{j,3}]
k22 = kcol22 + kcap;
MatrixForm[Simplify[N[k22]]]
```

$$\begin{pmatrix} 1.1302\times10^{6}+(0.+5351.75\,i)\,\omega & 0. & -2.0354\times10^{-11}-(0.+2.63775\times10^{-13}\,i)\,\omega \\ 0. & 442649.+(0.+3648.25\,i)\,\omega & -1.25636\times10^{6}-(0.+701.141\,i)\,\omega \\ -2.0354\times10^{-11}-(0.+2.63775\times10^{-13}\,i)\,\omega & -1.25636\times10^{6}-(0.+701.141\,i)\,\omega & 1.26712\times10^{7}+(0.+35133.3\,i)\,\omega \end{pmatrix}$$

```
Do[kij[i+3,j+3]=k22[[i,j]],{i,3},{j,3}]
```

Dynamic Stiffness (i.e., including inertia)

```
dynk=k-m ω^2;
```

Eigenvalue Solution

Determinant of the Dynamic Stiffness

```
cheqn=Det[dynk];
```

Eigenvalues

```
freq=Solve[cheqn==0,ω]
```

```
{{ω→-218.507+91.0289 i},{ω→-148.622+42.2174 i},{ω→-83.5602+42.7649 i},{ω→-
82.5748+59.1152 i},{ω→-58.0513+6.52529 i},{ω→-14.5608+0.914899 i},{ω→14.5608 +0.914899
i},{ω→58.0513 +6.52529 i},{ω→82.5748 +59.1152 i},{ω→83.5602 +42.7649 i},{ω→148.622
+42.2174 i},{ω→218.507 +91.0289 i}}
```

Fundamental Frequency

```
freq[[7]]
```

```
{ω→14.5608 +0.914899 i}
```

Dynamic Stiffness for the Fundamental Frequency

```
stiff1=dynk/.freq[[7]];
```

Eigenvector for the Fundamental Frequency

```
mShape=NullSpace[stiff1]
```

$$\{\{7.88635\times10^{-17}-1.22474\times10^{-17}\,i,\ 0.985276+0.129754\,i,\ -0.0946145-0.0150548\,i,\ 7.81532\times10^{-17}-1.22271\times10^{-17}\,i,\ 0.0105994+0.000877685\,i,\ -0.0555561-0.00413114\,i\}\}$$

Modal Amplitudes of the degrees of freedom at the Fundamental Frequency

```
Abs[mShape]
```

$$\{\{7.98089\times10^{-17},\ 0.993783,\ 0.0958048,\ 7.91039\times10^{-17},\ 0.0106357,\ 0.0557095\}\}$$

Phase angles of the degrees of freedom at the Fundamental Frequency

```
Arg[mShape]
```

```
{{-0.154068,0.130939,-2.9838,-0.155192,0.0826166,-3.06737}}
```

```
statStiff=k/.ω->0
```

$$\{\{717131.,\ 0,\ 0,\ -717131.,\ 0,\ 0\},\ \{0,\ 189714.,\ 1.19046\times10^{6},\ 0,\ -189714.,\ 1.19046\times10^{6}\},\ \{0,\ 1.19046\times10^{6},\ 9.96016\times10^{6},\ 0,\ -1.19046\times10^{6},\ 4.98008\times10^{6}\},\ \{-717131.,\ 0,\ 0,\ 1.1302\times10^{6},\ 0,\ -2.0354\times10^{-11}\},\ \{0,\ -189714.,\ -1.19046\times10^{6},\ 0,\ 442649.,\ -1.25636\times10^{6}\},\ \{0,\ 1.19046\times10^{6},\ 4.98008\times10^{6},\ -2.0354\times10^{-11},\ -1.25636\times10^{6},\ 1.26712\times10^{7}\}\}$$

```
LinearSolve[statStiff,{0,1000000,0,0,0,0}]
```

$$\{-2.24796\times10^{-16},\ 81.1026,\ -7.08206,\ -2.24796\times10^{-16},\ 2.76486,\ -4.56202\}$$

Similar process are followed for Batter angles such as 0^0, 5^0, 12^0, 14^0, 16^0, 18^0 and 20^0.

APPENDIX-F

Programming by MATLAB

In this study, pier-top deformation and pile-cap deformation have been conducted for various frequencies at different Batter angles such as 0^0, 5^0, 10^0, 15^0, and 20^0 using MATLAB software. Programming for 5^0 is as follows:

```
% batter_in

omega = 2*pi; %frequency

%Pile parameters

k_x = 13770+i*2801;
k_z = 22160+i*1541;
k_xphi = 23348+i*3604;
k_phi = 148064+i*7452;

npile = 18;
x = [-3.6; -3.6; -3.6; -2.6; -2.6; -1.5; -1.5; -1.5; 0; 0; 1.5; 1.5;
1.5; 2.6; 2.6; 3.6; 3.6; 3.6];
theta = pi/180*[-5; -5; -5; -5; -5; -5; -5; -5; 0; 0; 5; 5; 5; 5; 5;
5; 5; 5];

%Pier parameters

l = 12.3;
ea = 3.96*2.1*10^6;
ei = 24.17*2.1*10^6;
m = [30, 30, 3000, 20, 20, 1000];


%kinematic interaction factors

te_z = 0.9968+i*6.15*10^(-4);
te_x = 1.029-i*0.00314;
te_xphi = 0.01959-i*0.00257;
```

```
% batter_kine

batter_in

if length(x)~=npile || length(theta)~=npile
    error('length of x and theta must be equal to npile')
end

sub_stiff

super_stiff

kine_interact




%kine_interact

fcap_x = zeros(3,1);
fcap_z = zeros(3,1);

for ipile=1:npile
    fp1_x = [(k_x-k_z)*sin(theta(ipile))*cos(theta(ipile)) 0; ...
            k_z*sin(theta(ipile))^2+k_x*cos(theta(ipile))^2
k_xphi*cos(theta(ipile)); k_xphi*cos(theta(ipile)) k_phi]*[te_x;
te_xphi];
    fp1_z = te_z*[k_z*cos(theta(ipile))^2+k_x*sin(theta(ipile))^2;
...
            (k_x-k_z)*sin(theta(ipile))*cos(theta(ipile));
k_xphi*sin(theta(ipile))];
    fcap_x = fcap_x + fp1_x;
    fcap_x(3) = fcap_x(3) + x(ipile)*fp1_x(1);
    fcap_z = fcap_z + fp1_z;
    fcap_z(3) = fcap_z(3) + x(ipile)*fp1_z(1);
end

f_x = zeros(6,1);
f_z = zeros(6,1);
f_x(4:6) = fcap_x;
f_z(4:6) = fcap_z;

u_x = k\f_x;
u_xmod =abs(u_x)
u_xphase = angle(u_x)*180/pi
u_z = k\f_z;
u_zmod = abs(u_z);
u_zphase = angle(u_z)*180/pi;

u_cap = kcap\fcap_x;
u_capmod = abs(u_cap)
u_capphase = angle(u_cap)*180/pi
```

```
%kine_solve

f_super = -k(7:end,7:end)*u_p2;

u_super = k(1:6,1:6)\f_super




function k = kp(kx,kz,kxp,kp,theta)


kp = [kx*(sin(theta))^2+kz*(cos(theta)^2) (kx-
kz)*sin(theta)*cos(theta) kxp*sin(theta); ...
        (kx-kz)*sin(theta)*cos(theta)
kx*(cos(theta)^2)+kz*(sin(theta)^2) kxp*cos(theta); ...
        kxp*sin(theta) kxp*cos(theta) kp];







% sub_stiff

kcap=zeros(3);

for ipile=1:npile
    kp = [k_x*sin(theta(ipile))^2+k_z*cos(theta(ipile))^2 (k_x-
k_z)*sin(theta(ipile))*cos(theta(ipile)) k_xphi*sin(theta(ipile));
...
        (k_x-k_z)*sin(theta(ipile))*cos(theta(ipile))
k_x*cos(theta(ipile))^2+k_z*sin(theta(ipile))^2
k_xphi*cos(theta(ipile)); ...
        k_xphi*sin(theta(ipile)) k_xphi*cos(theta(ipile)) k_phi];

    kcap = kcap+kp;
    kcap(1,3) = kcap(1,3) + x(ipile) * (k_x*sin(theta(ipile))^2 +
k_z*cos(theta(ipile))^2);
    kcap(3,1) = kcap(1,3);
    kcap(2,3) = kcap(2,3) + x(ipile) * (k_x-
k_z)*sin(theta(ipile))*cos(theta(ipile));
    kcap(3,2) = kcap(2,3);
    kcap(3,3) = kcap(3,3) + x(ipile)^2 * (k_x*sin(theta(ipile))^2 +
k_z*cos(theta(ipile))^2);
```

```
end

kcap


%super_stiff

kcol = [ea/l 0 0 -ea/l 0 0; 0 12*ei/l^3 6*ei/l^2 0 -12*ei/l^3
6*ei/l^2; 0 6*ei/l^2 4*ei/l 0 -6*ei/l^2 2*ei/l; ...
        -ea/l 0 0 ea/l 0 0; 0 -12*ei/l*3 -6*ei/l^2 0 12*ei/l^3 -
6*ei/l^2; 0 6*ei/l^2 2*ei/l 0 -6*ei/l^2 4*ei/l]

k = kcol;

k(4:6,4:6) = k(4:6,4:6)+kcap

k = k - omega^2 * diag(m,0)
```

Out put by MATLAB at 05 º

>> batter_kine (0.5 Hz)

kcap =

1.0e+006 *

0.4128 + 0.0234i	0.0000 - 0.0000i	-0.0000 + 0.0000i
0.0000 - 0.0000i	0.2352 + 0.0220i	0.3591 + 0.0194i
-0.0000 + 0.0000i	0.3591 + 0.0194i	5.4119 + 0.2131i

kcol =

1.0e+008 *

0.0068	0	0	-0.0068	0	0
0	0.0033	0.0201	0	-0.0033	0.0201
0	0.0201	0.1651	0	-0.0201	0.0825
-0.0068	0	0	0.0068	0	0
0	-1.4856	-0.0201	0	0.0033	-0.0201
0	0.0201	0.0825	0	-0.0201	0.1651

k =

1.0e+008 *

0.0068	0	0	-0.0068	0	0
0	0.0033	0.0201	0	-0.0033	0.0201
0	0.0201	0.1651	0	-0.0201	0.0825
-0.0068	0	0	0.0109 + 0.0002i	0.0000 - 0.0000i	-0.0000 + 0.0000i
0	-1.4856	-0.0201	0.0000 - 0.0000i	0.0056 + 0.0002i	-0.0165 + 0.0002i
0	0.0201	0.0825	-0.0000 + 0.0000i	-0.0165 + 0.0002i	0.2192 + 0.0021i

k =

```
1.0e+008 *

  0.0068         0         0   -0.0068         0         0
       0    0.0033    0.0201         0   -0.0033    0.0201
       0    0.0201    0.1648         0   -0.0201    0.0825
  -0.0068         0         0   0.0109 + 0.0002i   0.0000 - 0.0000i  -0.0000 + 0.0000i
       0   -1.4856   -0.0201   0.0000 - 0.0000i   0.0056 + 0.0002i  -0.0165 + 0.0002i
       0    0.0201    0.0825  -0.0000 + 0.0000i  -0.0165 + 0.0002i   0.2191 + 0.0021i


u_xmod =

   0.0000
   0.0008
   0.0385
   0.0000
   0.4710
   0.0382


u_xphase =

  -18.2498
 -174.7817
    0.0822
  -18.2498
    0.0738
    0.0822


u_capmod =

   0.0000
   1.0118
   0.0021


u_capphase =

  176.7129
   -0.1119
   -8.1695

>> batter_kine (1.0 Hz)


kcap =

  1.0e+006 *

   0.3979 + 0.0279i   0.0000 - 0.0000i  -0.0000 + 0.0000i
   0.0000 - 0.0000i   0.2489 + 0.0503i   0.3890 + 0.0691i
  -0.0000 + 0.0000i   0.3890 + 0.0691i   5.2791 + 0.3176i


kcol =

  1.0e+008 *

   0.0068         0         0   -0.0068         0         0
        0    0.0033    0.0201         0   -0.0033    0.0201
        0    0.0201    0.1651         0   -0.0201    0.0825
```

```
  -0.0068         0         0    0.0068         0         0
         0   -1.4856   -0.0201         0    0.0033   -0.0201
         0    0.0201    0.0825         0   -0.0201    0.1651


k =

  1.0e+008 *

   0.0068         0         0   -0.0068         0         0
         0    0.0033    0.0201         0   -0.0033    0.0201
         0    0.0201    0.1651         0   -0.0201    0.0825
  -0.0068         0         0    0.0107 + 0.0003i   0.0000 - 0.0000i  -0.0000 + 0.0000i
         0   -1.4856   -0.0201    0.0000 - 0.0000i   0.0058 + 0.0005i  -0.0162 + 0.0007i
         0    0.0201    0.0825   -0.0000 + 0.0000i  -0.0162 + 0.0007i   0.2179 + 0.0032i


k =

  1.0e+008 *

   0.0067         0         0   -0.0068         0         0
         0    0.0033    0.0201         0   -0.0033    0.0201
         0    0.0201    0.1639         0   -0.0201    0.0825
  -0.0068         0         0    0.0107 + 0.0003i   0.0000 - 0.0000i  -0.0000 + 0.0000i
         0   -1.4856   -0.0201    0.0000 - 0.0000i   0.0058 + 0.0005i  -0.0162 + 0.0007i
         0    0.0201    0.0825   -0.0000 + 0.0000i  -0.0162 + 0.0007i   0.2175 + 0.0032i


u_xmod =

    0.0000
    0.0007
    0.0470
    0.0000
    0.5686
    0.0456


u_xphase =

   -52.5245
  -171.8654
     1.5071
   -52.5245
     1.4985
     1.5069


u_capmod =

    0.0000
    1.0485
    0.0085


u_capphase =

   174.3503
    -0.3606
    -8.8313
```

>> batter_kine (2.0 Hz)

kcap =

1.0e+006 *

0.3879 + 0.0872i 0 - 0.0000i 0.0000 - 0.0000i
0 - 0.0000i 0.2493 + 0.0676i 0.4051 + 0.0808i
0.0000 - 0.0000i 0.4051 + 0.0808i 5.2425 + 0.7330i

kcol =

1.0e+008 *

0.0068 0 0 -0.0068 0 0
0 0.0033 0.0201 0 -0.0033 0.0201
0 0.0201 0.1651 0 -0.0201 0.0825
-0.0068 0 0 0.0068 0 0
0 -1.4856 -0.0201 0 0.0033 -0.0201
0 0.0201 0.0825 0 -0.0201 0.1651

k =

1.0e+008 *

0.0068 0 0 -0.0068 0 0
0 0.0033 0.0201 0 -0.0033 0.0201
0 0.0201 0.1651 0 -0.0201 0.0825
-0.0068 0 0 0.0106 + 0.0009i 0 - 0.0000i 0.0000 - 0.0000i
0 -1.4856 -0.0201 0 - 0.0000i 0.0058 + 0.0007i -0.0161 + 0.0008i
0 0.0201 0.0825 0.0000 - 0.0000i -0.0161 + 0.0008i 0.2175 + 0.0073i

k =

1.0e+008 *

0.0067 0 0 -0.0068 0 0
0 0.0032 0.0201 0 -0.0033 0.0201
0 0.0201 0.1603 0 -0.0201 0.0825
-0.0068 0 0 0.0106 + 0.0009i 0 - 0.0000i 0.0000 - 0.0000i
0 -1.4856 -0.0201 0 - 0.0000i 0.0057 + 0.0007i -0.0161 + 0.0008i
0 0.0201 0.0825 0.0000 - 0.0000i -0.0161 + 0.0008i 0.2159 + 0.0073i

u_xmod =

0.0000
0.0005
0.0729
0.0000
0.8445
0.0645

u_xphase =

145.5249
-156.0499
-3.2854

```
  145.5249
   -3.3008
   -3.2868


u_capmod =

    0.0000
    1.1588
    0.0325


u_capphase =

  140.5136
   -0.0603
  -12.7393

>> batter_kine(2.5 Hz)

kcap =

  1.0e+006 *

   0.4029 + 0.1078i   0.0000 - 0.0000i        0 + 0.0000i
   0.0000 - 0.0000i   0.2498 + 0.0755i   0.4140 + 0.0875i
       0 + 0.0000i   0.4140 + 0.0875i   5.3563 + 0.8820i


kcol =

  1.0e+008 *

    0.0068         0         0   -0.0068         0         0
         0    0.0033    0.0201         0   -0.0033    0.0201
         0    0.0201    0.1651         0   -0.0201    0.0825
   -0.0068         0         0    0.0068         0         0
         0   -1.4856   -0.0201         0    0.0033   -0.0201
         0    0.0201    0.0825         0   -0.0201    0.1651


k =

  1.0e+008 *

   0.0068              0              0         -0.0068              0              0
        0         0.0033         0.0201              0         -0.0033         0.0201
        0         0.0201         0.1651              0         -0.0201         0.0825
  -0.0068              0              0          0.0108 + 0.0011i   0.0000 - 0.0000i        0 + 0.0000i
        0        -1.4856        -0.0201          0.0000 - 0.0000i   0.0058 + 0.0008i  -0.0160 + 0.0009i
        0         0.0201         0.0825              0 + 0.0000i  -0.0160 + 0.0009i   0.2186 + 0.0088i


k =

  1.0e+008 *

   0.0067              0              0         -0.0068              0              0
        0         0.0032         0.0201              0         -0.0033         0.0201
        0         0.0201         0.1577              0         -0.0201         0.0825
  -0.0068              0              0          0.0107 + 0.0011i   0.0000 - 0.0000i        0 + 0.0000i
        0        -1.4856        -0.0201          0.0000 - 0.0000i   0.0057 + 0.0008i  -0.0160 + 0.0009i
```

```
      0         0.0201         0.0825              0 + 0.0000i  -0.0160 + 0.0009i   0.2162 + 0.0088i


u_xmod =

   0.0000
   0.0003
   0.0799
   0.0000
   0.8944
   0.0655


u_xphase =

 -125.1110
    1.3412
    3.6357
 -125.1110
    3.6350
    3.6356


u_capmod =

   0.0000
   0.7247
   0.0655


u_capphase =

 -121.6256
    8.5694
    1.8903

>> batter_kine (3.0 Hz)

kcap =

  1.0e+006 *

   0.4142 + 0.1193i  -0.0000 - 0.0000i   0.0000 - 0.0000i
  -0.0000 - 0.0000i   0.2527 + 0.0923i   0.4199 + 0.1022i
   0.0000 - 0.0000i   0.4199 + 0.1022i   5.4349 + 0.9676i


kcol =

  1.0e+008 *

   0.0068         0         0   -0.0068         0         0
        0    0.0033    0.0201         0   -0.0033    0.0201
        0    0.0201    0.1651         0   -0.0201    0.0825
  -0.0068         0         0    0.0068         0         0
        0   -1.4856   -0.0201         0    0.0033   -0.0201
        0    0.0201    0.0825         0   -0.0201    0.1651


k =

  1.0e+008 *
```

```
  0.0068         0         0   -0.0068         0         0
       0    0.0033    0.0201         0   -0.0033    0.0201
       0    0.0201    0.1651         0   -0.0201    0.0825
  -0.0068         0         0   0.0109 + 0.0012i  -0.0000 - 0.0000i   0.0000 - 0.0000i
       0   -1.4856   -0.0201     -0.0000 - 0.0000i   0.0058 + 0.0009i  -0.0159 + 0.0010i
       0    0.0201    0.0825      0.0000 - 0.0000i  -0.0159 + 0.0010i   0.2194 + 0.0097i


k =

  1.0e+008 *

  0.0067         0         0   -0.0068         0         0
       0    0.0032    0.0201         0   -0.0033    0.0201
       0    0.0201    0.1544         0   -0.0201    0.0825
  -0.0068         0         0   0.0108 + 0.0012i  -0.0000 - 0.0000i   0.0000 - 0.0000i
       0   -1.4856   -0.0201     -0.0000 - 0.0000i   0.0057 + 0.0009i  -0.0159 + 0.0010i
       0    0.0201    0.0825      0.0000 - 0.0000i  -0.0159 + 0.0010i   0.2159 + 0.0097i


u_xmod =

    0.0000
    0.0003
    0.1170
    0.0000
    1.2534
    0.0868


u_xphase =

   73.1408
  -42.6751
   -3.1496
   73.1408
   -3.1574
   -3.1513


u_capmod =

    0.0000
    1.1956
    0.0651


u_capphase =

   64.6621
    3.3771
   -7.8923

>> batter_kine (3.5 Hz)

kcap =

  1.0e+006 *

   0.4239 + 0.1285i   0.0000           -0.0000 - 0.0000i
   0.0000             0.2592 + 0.1008i   0.4309 + 0.1112i
```

```
 -0.0000 - 0.0000i   0.4309 + 0.1112i   5.5103 + 1.0183i


kcol =

 1.0e+008 *

   0.0068         0         0   -0.0068         0         0
        0    0.0033    0.0201         0   -0.0033    0.0201
        0    0.0201    0.1651         0   -0.0201    0.0825
  -0.0068         0         0    0.0068         0         0
        0   -1.4856   -0.0201         0    0.0033   -0.0201
        0    0.0201    0.0825         0   -0.0201    0.1651


k =

 1.0e+008 *

   0.0068              0              0        -0.0068              0              0
        0         0.0033         0.0201              0        -0.0033         0.0201
        0         0.0201         0.1651              0        -0.0201         0.0825
  -0.0068              0              0         0.0110 + 0.0013i   0.0000        -0.0000 - 0.0000i
        0        -1.4856        -0.0201              0         0.0059 + 0.0010i  -0.0158 + 0.0011i
        0         0.0201         0.0825        -0.0000 - 0.0000i  -0.0158 + 0.0011i   0.2202 + 0.0102i


k =

 1.0e+008 *

   0.0066              0              0        -0.0068              0              0
        0         0.0031         0.0201              0        -0.0033         0.0201
        0         0.0201         0.1506              0        -0.0201         0.0825
  -0.0068              0              0         0.0109 + 0.0013i   0.0000        -0.0000 - 0.0000i
        0        -1.4856        -0.0201              0         0.0058 + 0.0010i  -0.0158 + 0.0011i
        0         0.0201         0.0825        -0.0000 - 0.0000i  -0.0158 + 0.0011i   0.2153 + 0.0102i


u_xmod =

   0.0000
   0.0003
   0.1268
   0.0000
   1.2858
   0.0822


u_xphase =

   48.3069
  -25.7947
   -3.8553
   48.3069
   -3.8602
   -3.8568


u_capmod =

   0.0000
```

```
   1.1947
   0.0512


u_capphase =

   51.1013
    1.3872
   -4.8342

>> batter_kine (4.0 Hz)

kcap =

  1.0e+006 *

   0.4323 + 0.1360i        0            -0.0000 + 0.0000i
        0             0.2631 + 0.1072i   0.4418 + 0.1173i
  -0.0000 + 0.0000i   0.4418 + 0.1173i   5.5738 + 1.1101i


kcol =

  1.0e+008 *

    0.0068         0         0   -0.0068         0         0
         0    0.0033    0.0201         0   -0.0033    0.0201
         0    0.0201    0.1651         0   -0.0201    0.0825
   -0.0068         0         0    0.0068         0         0
         0   -1.4856   -0.0201         0    0.0033   -0.0201
         0    0.0201    0.0825         0   -0.0201    0.1651


k =

  1.0e+008 *

   0.0068              0              0         -0.0068              0              0
        0         0.0033         0.0201              0         -0.0033         0.0201
        0         0.0201         0.1651              0         -0.0201         0.0825
  -0.0068              0              0    0.0111 + 0.0014i         0    -0.0000 + 0.0000i
        0        -1.4856        -0.0201              0    0.0059 + 0.0011i  -0.0157 + 0.0012i
        0         0.0201         0.0825    -0.0000 + 0.0000i  -0.0157 + 0.0012i   0.2208 + 0.0111i


k =

  1.0e+008 *

   0.0066              0              0         -0.0068              0              0
        0         0.0031         0.0201              0         -0.0033         0.0201
        0         0.0201         0.1461              0         -0.0201         0.0825
  -0.0068              0              0    0.0110 + 0.0014i         0    -0.0000 + 0.0000i
        0        -1.4856        -0.0201              0    0.0058 + 0.0011i  -0.0157 + 0.0012i
        0         0.0201         0.0825    -0.0000 + 0.0000i  -0.0157 + 0.0012i   0.2145 + 0.0111i


u_xmod =

   0.0000
   0.0010
   0.1631
```

```
    0.0000
    1.5467
    0.0882


u_xphase =

  -32.2747
    0.8584
   -4.2139
  -32.2747
   -4.2101
   -4.2122


u_capmod =

    0.0000
    1.0102
    0.0706


u_capphase =

  -29.2162
    6.0566
   -3.4960

>> batter_kine (5.0 Hz)

kcap =

  1.0e+006 *

   0.4464 + 0.1492i  -0.0000 - 0.0000i  -0.0000 + 0.0000i
  -0.0000 - 0.0000i   0.2676 + 0.1247i   0.4599 + 0.1271i
  -0.0000 + 0.0000i   0.4599 + 0.1271i   5.6853 + 1.2286i


kcol =

  1.0e+008 *

    0.0068         0         0   -0.0068         0         0
         0    0.0033    0.0201         0   -0.0033    0.0201
         0    0.0201    0.1651         0   -0.0201    0.0825
   -0.0068         0         0    0.0068         0         0
         0   -1.4856   -0.0201         0    0.0033   -0.0201
         0    0.0201    0.0825         0   -0.0201    0.1651


k =

  1.0e+008 *

    0.0068              0              0         -0.0068              0              0
         0         0.0033         0.0201              0         -0.0033         0.0201
         0         0.0201         0.1651              0         -0.0201         0.0825
   -0.0068              0              0    0.0112 + 0.0015i  -0.0000 - 0.0000i  -0.0000 + 0.0000i
         0        -1.4856        -0.0201   -0.0000 - 0.0000i   0.0059 + 0.0012i  -0.0155 + 0.0013i
         0         0.0201         0.0825   -0.0000 + 0.0000i  -0.0155 + 0.0013i   0.2219 + 0.0123i
```

k =

1.0e+008 *

0.0065	0	0	-0.0068	0	0
0	0.0030	0.0201	0	-0.0033	0.0201
0	0.0201	0.1355	0	-0.0201	0.0825
-0.0068	0	0	0.0110 + 0.0015i	-0.0000 - 0.0000i	-0.0000 + 0.0000i
0	-1.4856	-0.0201	-0.0000 - 0.0000i	0.0058 + 0.0012i	-0.0155 + 0.0013i
0	0.0201	0.0825	-0.0000 + 0.0000i	-0.0155 + 0.0013i	0.2120 + 0.0123i

u_xmod =

0.0000
0.0030
0.2880
0.0000
2.2753
0.0815

u_xphase =

-77.7110
-0.9292
-16.0967
-77.7110
-16.0731
-16.0721

u_capmod =

0.0000
0.7325
0.0601

u_capphase =

-65.6415
7.2140
1.0610

Similar process are followed for various frequencies at Batter angles such as 0^0, 10^0, 15^0, and 20^0